Hardin, R.A., and Beckermann, C., "Validation and Gage R&R Studies of a New Radiography Standard for Steel Castings," in Proceedings of the 64th SFSA Technical and Operating Conference, Paper No. 2.6, Steel Founders' Society of America, Chicago, IL, 2010.

Validation and Gage R&R Studies of a New Radiography Standard for Steel Castings

Richard A. Hardin and Christoph Beckermann

Department of Mechanical and Industrial Engineering
The University of Iowa, Iowa City, IA 52242

Abstract

This paper presents two studies of a new radiography standard. In Part I, a validation study of a proposed relationship between radiographic testing (RT) acceptance criteria and the mechanical performance of a casting in tension is performed. In the validation study, the new RT standard is used to measure and rate radiographic indications in WCB steel tensile test plates. Then the radiographic testing results are compared to measured tensile properties. The tensile plate castings all contained porosity and their maximum indication fractions were from 40% to 60%. This corresponds roughly to RT Level 4 to 5. It is found that the stiffness of the plate castings ranged from 72% to 95% of sound material, with an average of 88% of sound material. The yield stress is not reduced on average for the tensile test plates, and ranged from 92% to 109% of the sound yield stress. The ultimate tensile strength also changed little from the sound material. Ductility in the test castings was markedly reduced with the percent elongation data ranging from 12.8% to 19.6%; versus 22% elongation measured in the sound material. In Part II, a gage repeatability and reproducibility study of the revised new radiography standard is performed. The standard was revised following recommendations resulting from the gage R&R study presented at last years' SFSA T&O Conference. In the current gage R&R study, three radiographs are rated three times each by five evaluators. The largest source of error in the gage R&R study is the reader-to-reader reproducibility. However, it was reduced by 46% on average compared to last years gage R&R study. The error due to reader repeatability was reduced by an average of 30% from the previous study. Compared to the current ASTM RT standards, which have been shown to have an average confidence interval of ±1.4 levels, the revised new RT standard gives confidence intervals of ±0.17, ±0.38, and ±0.11 levels for the three radiographs evaluated in the study.

I. INTRODUCTION

Two years ago, at the SFSA Technical and Operating Conference, a new radiographic inspection standard for steel castings was first presented [1]. This standard was developed jointly by the SFSA and the Solidification Laboratory at the University of Iowa. It was designed to provide both a quantitative measure of the internal soundness of a casting and a method for relating this to service performance. The need for this new standard originates from the deficiencies of the current ASTM radiographic testing (RT) standards (ASTM E186, E280, E446). Their main deficiencies are their subjectivity and their inability to provide any relationship between rating level and casting performance in service.

In the current ASTM RT standards, the x-ray "reader" makes a subjective decision on the corresponding type and level of indication severity in the test radiograph by comparing it to standard radiographs. In this comparison, the reader is told to prorate the area of interest on the test radiograph to the reference radiograph, and disregard gray level. These are two of the sources of reader-to-reader variability inherent in the current standards. It was demonstrated in a gage repeatability and reproducibility (R&R) study that readers have difficulty distinguishing the rating levels [2]. The average confidence interval from this gage R&R study of 128 radiographs was ±1.4 levels. Another important source of the variability is the reference radiographs themselves. Image analysis has shown that there are significant quantitative similarities between the levels of the ASTM E186 reference radiographs [2].

In the new standard, the severity level for a radiograph is determined from the measurement of the largest total length of individual indication lengths (l_{im}) on the radiograph along a specified direction, which is divided by a feature length **(L_f)** to arrive at the largest fractional length (l_{im} $/L_f$). This fractional length is termed the maximum indication fraction F ($F = l_{im} /L_f$). The specified direction is termed the "direction of interest" (DOI), and would be specified by the casting designer. The largest fractional length found is compared with an acceptance criterion, a maximum allowable fractional length, which is also specified by the designer of the casting. It is up to the designer to make their own assumptions about the effects of the radiographic indications on performance in specifying the DOI, the feature length and the maximum allowable fractional length. By making the assumptions more or less conservative, the designer can use the standard to ensure that the indications present on the radiographic film will not limit the component performance to less than the designer's requirements.

In the "Results Part I" section of the current paper, we present a study validating a relationship between the RT acceptance criteria and mechanical performance. To accomplish this, 0.75" thick plate test coupons were machined from 1"T x 5"W x 15"L and 18"L cast WCB plates. The test coupons were radiographed and rated according to the new revised RT standard, and were then pulled in tensile tests according to ASTM E8. It will be demonstrated that the assumptions made for this tensile loading case, relating the effects of porosity on the tensile behavior and the radiographic rating of test plate coupons, are conservative.

In "Results Part II", a gage R&R study is presented using the revised version of the new RT standard. The standard was revised following recommendations made after the gage R&R study using the standard that was presented at last years' T&O conference [3]. In order to understand these revisions and the reasons for them, the standard and results of last years' gage R&R are briefly reviewed. Then the results of the current gage R&R study will be compared with the previous study to demonstrate the degree of improvement observed using the revised standard.

II. PROCEDURES

Revised New Standard Procedure for Radiograph Rating

The procedure used to apply the revised new RT standard is given below, taken from the standard itself. From section 6 of [4]:

6. Procedure for Evaluation

6.1 All relevant indications present within the area of interest on a radiographic film shall be evaluated. The radiographic density of indications in comparison with the background density (i.e., the contrast) shall not be taken into account when evaluating indications.

6.2 The length (l_i) of an indication shall be measured along a straight line that is oriented in the direction of interest. The straight line shall have a width of 1/4th in (6.4 mm).

6.3 The total indication length for a single straight line shall be determined by summing the lengths of all indications along the line.

6.4 The maximum total indication length (l_{im}) shall be determined by finding the largest value of the total indication length for any duly oriented single straight line within the area of interest.

6.5 The maximum indication fraction (F) shall be calculated by dividing the maximum total indication length (l_{im}) by the specified feature length (L_f): $F = l_{im} / L_f$.

In 6.1 above, relevant indications are indications exceeding 1/16th inch (1.6 mm) in length. Also, no distinction is made between different types of discontinuities (porosity, holes, shrinkage, inclusions, etc.). Cracks, defined as an indication on the radiographic film with a length that exceeds 10 times the width, are unacceptable. The RT evaluation is made on an area of interest specified in the order, and this area may be just a portion of, or the entire test radiograph.

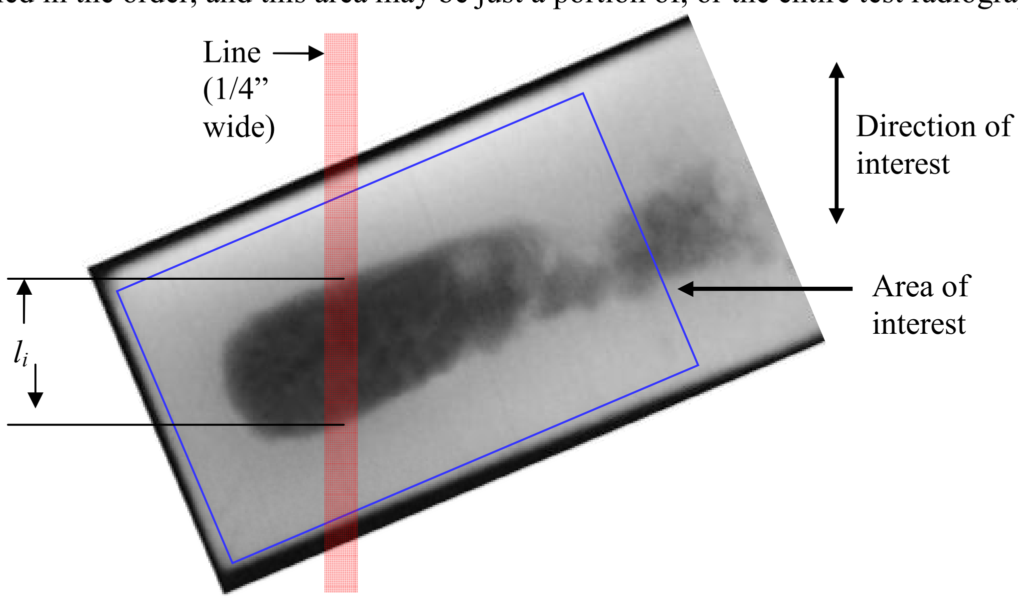

Figure 1. Example of the measurement of an indication length.

Consider the example given in Figure 1, where the specified direction of interest does not match the orientation of the edges of the radiograph. Here the radiograph is oriented such that the direction of interest is in the vertical direction. In practice, the direction of interest could be included on the radiographic film by placing an oriented lead wire on the casting section to be radiographed. As specified in Section 6.2 of the standard, the straight line in Figure 1 has a width of 1/4th inch. The maximum extent of an indication within this "strip" constitutes an indication length, l_i. In practice, it is recommended to perform the measurement using a transparent ruler that has a width of $1/4^{th}$ inch.

In Figure 1 there is a single indication, and the measured indication length represents the total indication length for this placement of the straight line. The maximum total indication length, l_{im}, is obtained by shifting the straight line horizontally, in order to keep it oriented in the direction of interest, until the maximum value of the indication length, within in the area of interest, is obtained. The placement of the straight line in Figure 1 corresponds approximately to this maximum value. If the straight line were shifted to the left or the right, a smaller indication length would be measured. Note that the direction of interest matters. For example, the maximum total indication length would be much larger if the direction of interest in Figure 1 were horizontal rather than vertical.

Not all indications are as easy to measure as those shown in Figure 1. In Figure 2, for example, the indications are generally long and narrow (as in centerline shrinkage) and have widely varying radiographic densities. This example illustrates why the straight line is taken to be 1/4th inch wide. If the straight line were of vanishing width, the indication length measurement would be very sensitive to the angle of the almost linear indication with respect to the direction of interest, as demonstrated in Figure 3. The use of the 0.25" strip was one important change made to the new standard arising from last years' gage R&R study.

In addition to using a $1/4^{th}$ inch strip, there were two other important revisions made to the new standard. From the previous, gage R&R study [3] it was apparent that some participants in the study focused on or only included darker indications in their measurements, disregarding the lighter indications. Hence, this text was added, "The radiographic density of indications in comparison with the background density (i.e., the contrast) shall not be taken into account when evaluating indications," for emphasis. In the third area of revision, the earlier version of the new standard included instructions that, "if the distance between two indication lengths is smaller

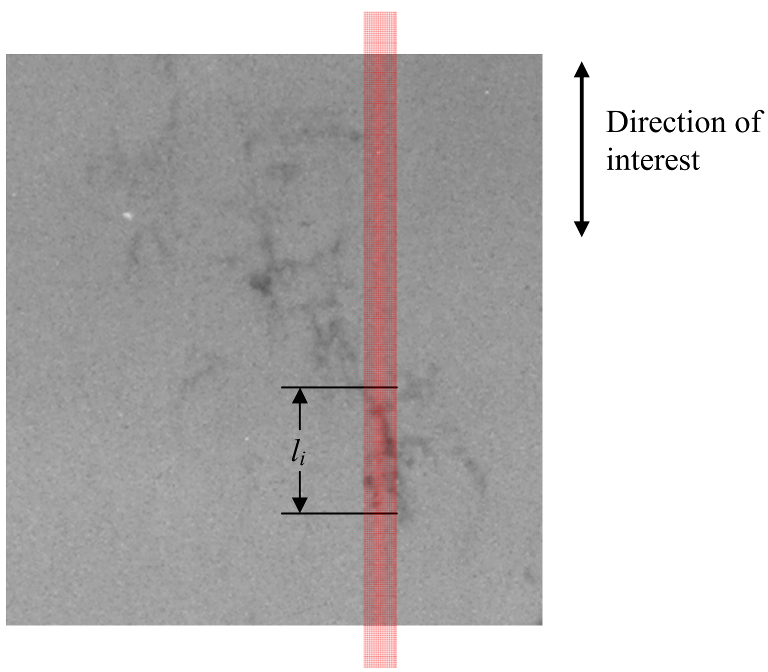

Figure 2. Example of the measurement of indication length for a long and narrow indication that is oriented close to the direction of interest.

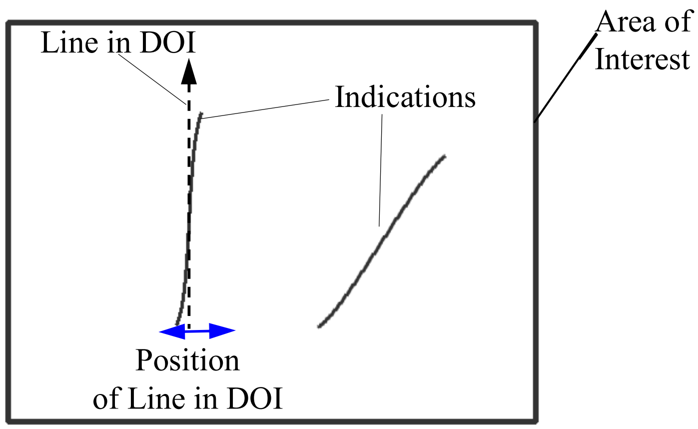

Figure 3. Demonstration that measurements of indications aligned in the direction of interest (DOI) are sensitive to the position of the line. Indication on left side is more sensitive to the position than that on the right.

than the length of the smaller indication, then the two indications, together with the space between the indications, are treated as a single indication." It was determined from the gage R&R study [3] that this instruction was difficult to follow and apply with consistency. So it was removed. The instructions are now simplified; each relevant indication is measured and all indications along the line in the DOI are summed to arrive at the total indication length.

Revised New Standard Acceptance Criteria for Radiograph Rating

Also arising from the gage R&R study done last year [3], the acceptance criteria section of the new standard was revised. This section of the revised standard [4] is given below. The change made was to account for reproducibility in the evaluation by adding a 1/16th of an inch to the acceptable maximum total indication length (l_{im}) for the levels of acceptable maximum indication fraction (F, where $F = l_{im} / L_f$) as shown in Table 1 below. The acceptance criteria section from [4] now is:

7. Acceptance Criteria
7.1 Cracks are unacceptable.

7.2 Maximum indication fractions exceeding the limit in Table 1 for a specified acceptance level are unacceptable.

Table 1. Acceptance criteria maximum indication fraction limits.

Acceptance Level	Level I	Level II	Level III	Level IV	Level V
F Limit	$F = 0.1$	$F = 0.2$	$F = 0.3$	$F = 0.4$	$F = 0.5$

7.3 In the case of a quality check after the casting has been certified, the acceptable maximum total indication length (l_{im}) for the levels of Table 1 shall be increased by 1/16th inch (1.6 mm) to account for reproducibility in the evaluation.

Procedure for Validation Study and Tensile Testing of Plates with Porosity

In the first part of the Results section of this paper, the results of a study validating a proposed relationship between the RT acceptance criteria and mechanical performance are presented. The relationship being validated is for a casting section in tension and is shown in Figure 4. The relationship assumes that the radiographic indications correspond to voids inside the casting. These voids reduce the stiffness and load-carrying ability of the casting section. The amount of the reduction is controlled by the maximum lost cross-sectional area, A_{im}, due to the voids in a plane perpendicular to the direction of the loading. It can be safely assumed that smaller voids along the loading direction, either in front or behind the plane with the maximum lost cross-sectional area, have no effect on the overall stiffness and load-carrying ability of the section. In other words, the weakest section will fail first. Therefore, acting under this worst case assumption that an indication is a void through the entire plate thickness, the maximum indication fraction corresponds to the ratio of the maximum void area A_{im} to sound cross-sectional area A, i.e., $F = A_{im}/A$. This results in the effective stiffness (elastic modulus, E) and load-carrying ability (yield strength, σ_y), normalized by the sound values, decreasing linearly with the maximum indication fraction, F. For example, if the maximum lost cross-sectional area

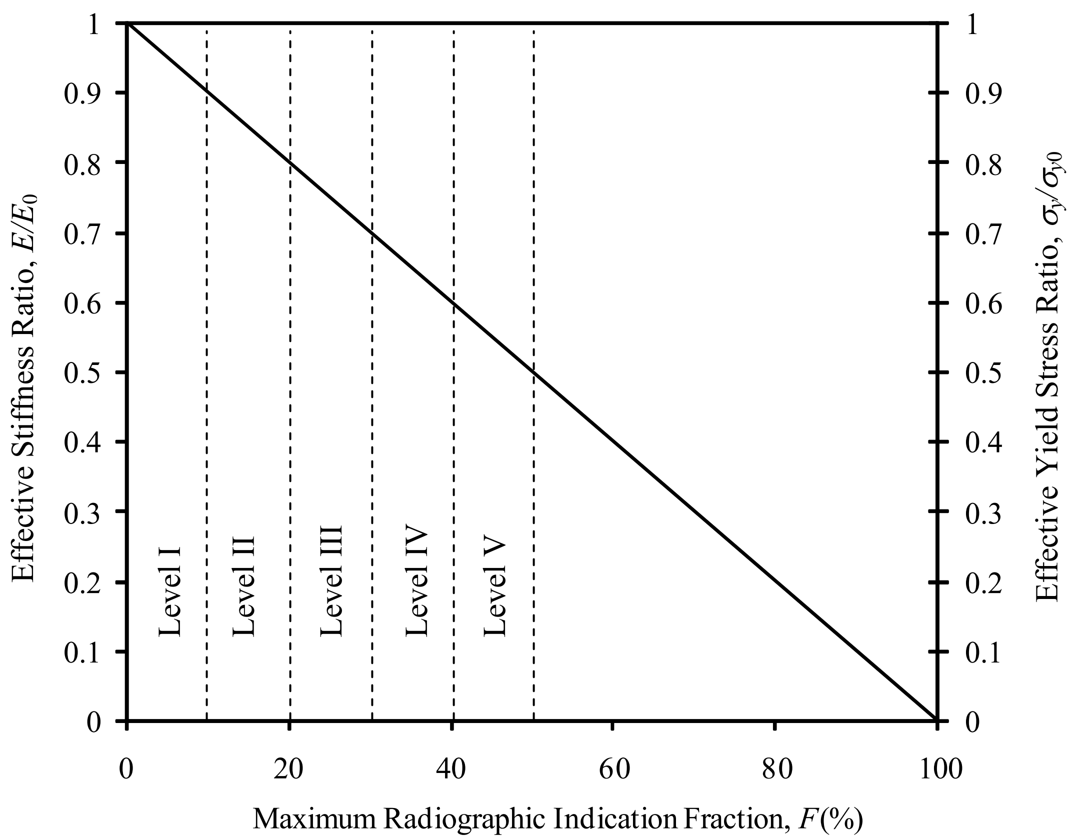

Figure 4. Proposed relationship between effective mechanical properties and the maximum radiographic indication fraction, F. Properties are normalized with their sound values, E_0 and σ_{y0}.

is 15% of the total cross-sectional area (F = 0.15), the section would retain 85% of its stiffness and load-carrying ability; according to Table 1, a value of F = 0.15 would correspond to a Level II casting section.

To validate the relationship in Figure 4, 0.75" thick plate test coupons were machined from 1"T x 5"W x 15"L cast ASTM A216 WCB plates having porosity. The plates were normalized at Sivyer Steel Casting in Bettendorf, Iowa prior to machining. Example radiographs of a cast plate and machined test coupon are shown in Figure 5. The dimensions for the test coupons were determined according to ASTM E8 tensile test standard [5] and are shown in Figure 6. Two small specimens were also machined from the plate castings from an end-effected zone to provide the sound property values, E_0 and σ_{y0}. Film and digital radiographs of the small sound specimens and unsound 0.75" thick coupons were made at Alloyweld Inspection, Bensenville, IL. The film radiographs were rated according to the revised new RT standard by Kent Carlson and Richard Hardin in the Solidification Laboratory at the University of Iowa. There was excellent agreement between their measurements of the maximum indication fraction F. The test coupon gage section width was used as the feature length L_f. The tensile testing was performed according to ASTM E8; for the sound specimens at University of Iowa, and for the ten 0.75" thick plates at SSAB North American Division, Muscatine, Iowa. In this work, it was important to have a large enough test plate with porosity so that the porosity would not result in large stress redistributions during testing. Also, test results for 0.75" thick plates are more representative of the behavior of an actual casting. Therefore it was important to have access to a large tensile

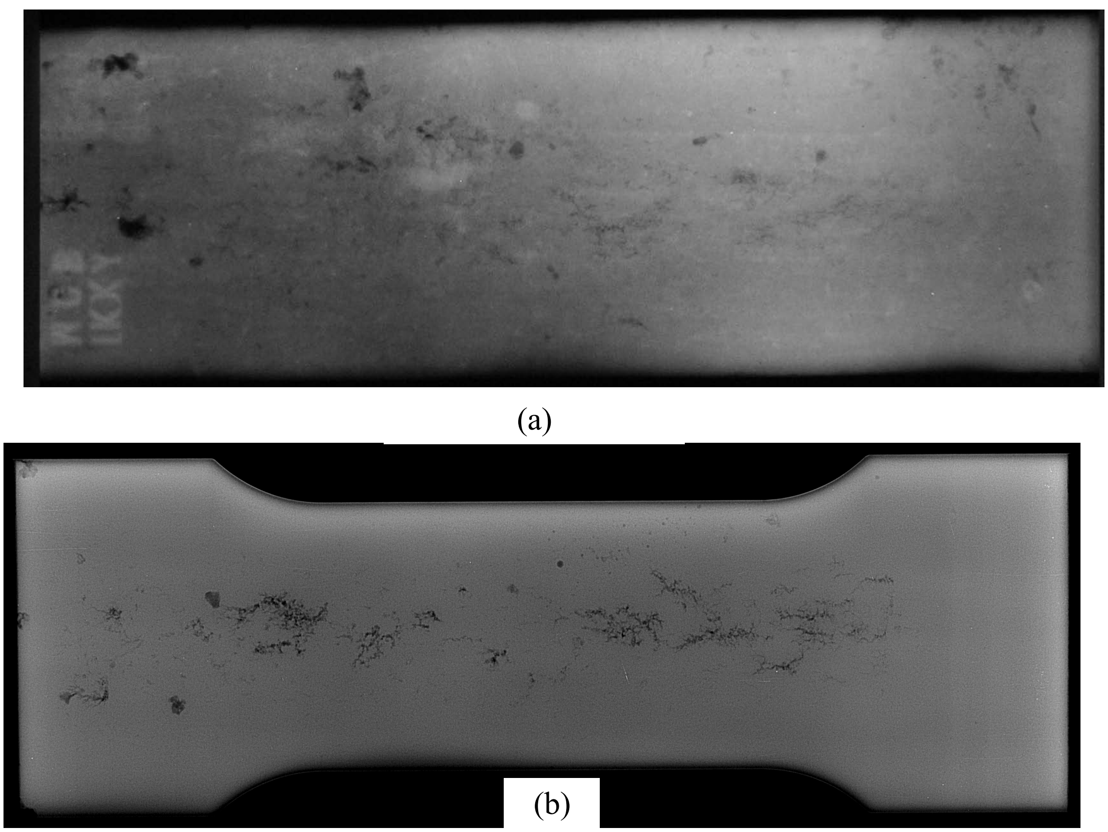

(a)

(b)

Figure 5. Radiographs of (a) as-cast plate, and (b) machined ¾" thick test coupon used in validation study.

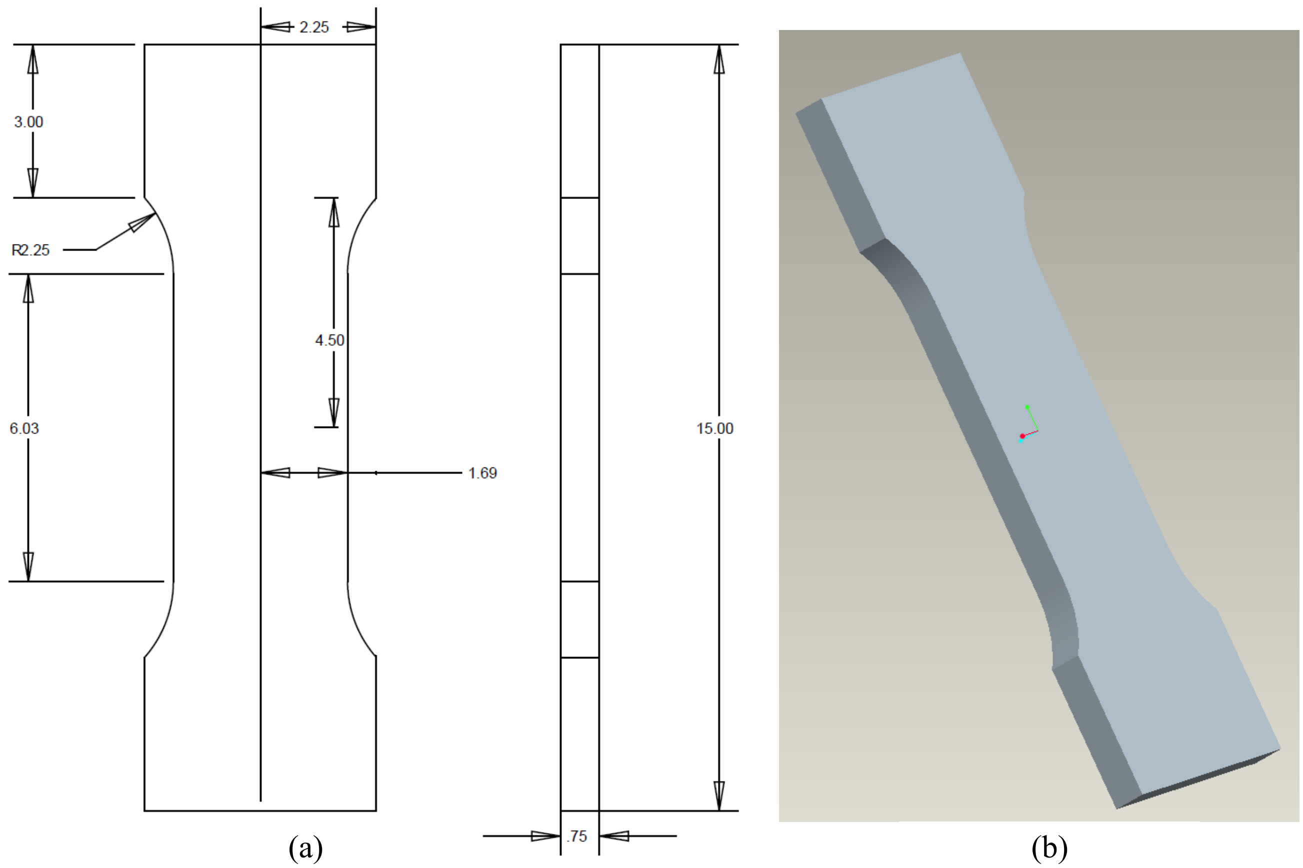

(a) (b)

Figure 6. (a) Dimensions (inches) and (b) rendering of machined test coupon used in validation study.

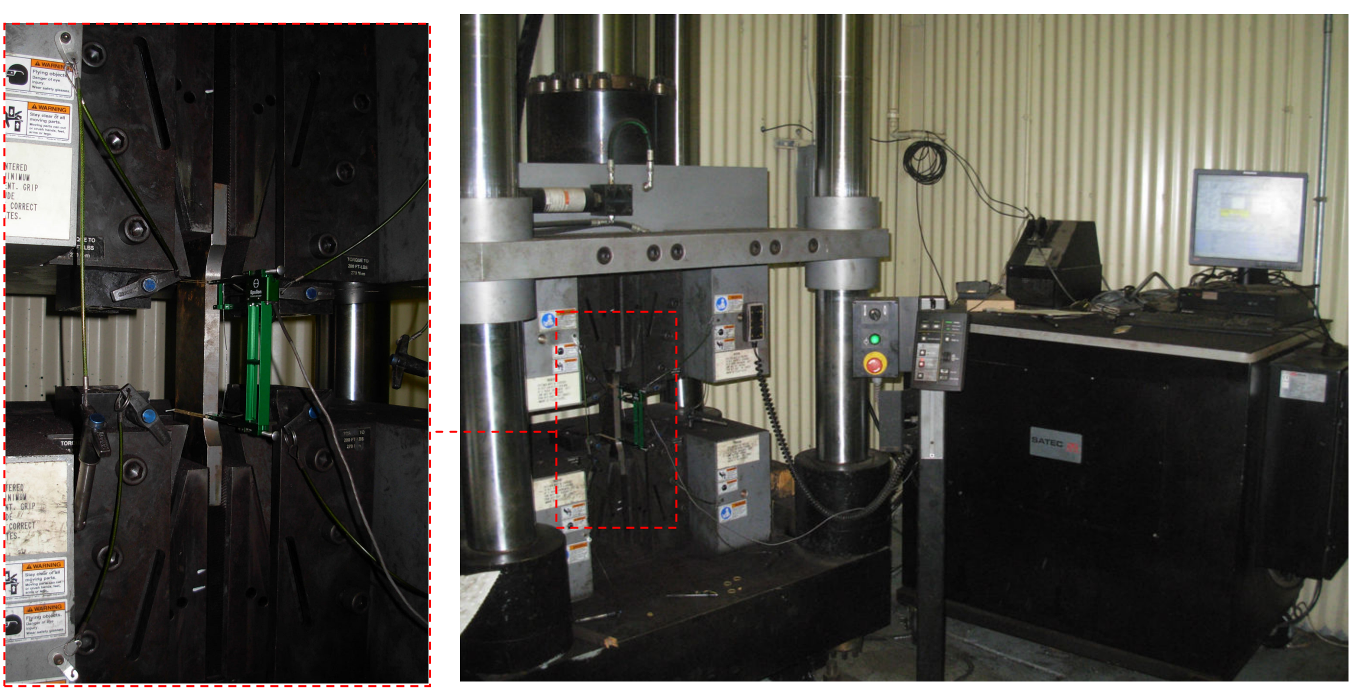

Figure 7. Close-up view of test coupon with 6” extensometer fixed to narrow face (image at left) and test machine and controller (image at right).

testing machine. As shown in Figure 7, an Instron 3500KN (800,000 lb) Tensile Test machine with Instron 5500 Control Unit controlled by Instron Partner Software was used at SSAB to perform the tests. Note in Figure 7 that the 6" extensometer had to be mounted on the narrow face (thickness edge) of the test coupons because of the configuration of the machine and grips.

Procedure for Gage R&R Study of Revised Radiographic Standard

The purpose of the gage R&R was to measure the variability in the measurements and ratings resulting from applying the revised standard. In the current study errors due to reproducibility and repeatability errors are calculated [6]. In addition, analysis of variance (ANOVA) is used to test whether the proportion of the "between readers" variation to "within all readers" variation is statistically significant [7]. The method of data reduction used in this study are identical to that given in detail in the 2009 study [3], and will not be repeated here. Please refer to the earlier gage R&R study for those details.

Factors affecting variability in applying the new standard are:

- Measurement device (ruler) used: 1/16th inch resolution, does it obscure the indications and is it kept aligned with the DOI?

- Reader-to-reader variability or "operator error": a reader's (or evaluator's) ability to make accurate measurements, read, understand and follow the standard.

- How measurements are made: alignment of measurement device, lighting of the radiographs and room used, fixture used for radiographs and measurement devices, how the data is recorded.

- Radiographs themselves: some are easier to read than others, rating can be sensitive to the alignment of the indications relative to the DOI, also it can be difficult to disregard the relative grey levels of the indications.

The goal here is to establish the overall repeatability and reproducibility errors resulting from typical applications of the revised standard and compare them with the results from the 2009 study [3]. In this study, five members of the Solidification Laboratory at the University of Iowa evaluated three radiographs according to the new standard. Each radiograph was evaluated three times measuring maximum indication lengths and recording their positions. In this study the radiograph width direction was used as the direction of interest and the width dimension was used as the feature length L_f.

III. RESULTS

Results Part I: Validation Study of a Proposed Relationship between RT Acceptance Criteria and Mechanical Performance

The radiographs of each plate tested in the validation study, and photographs of the plate taken after tensile testing are shown in Figures 8 through 17. The ten plates are identified by a letter

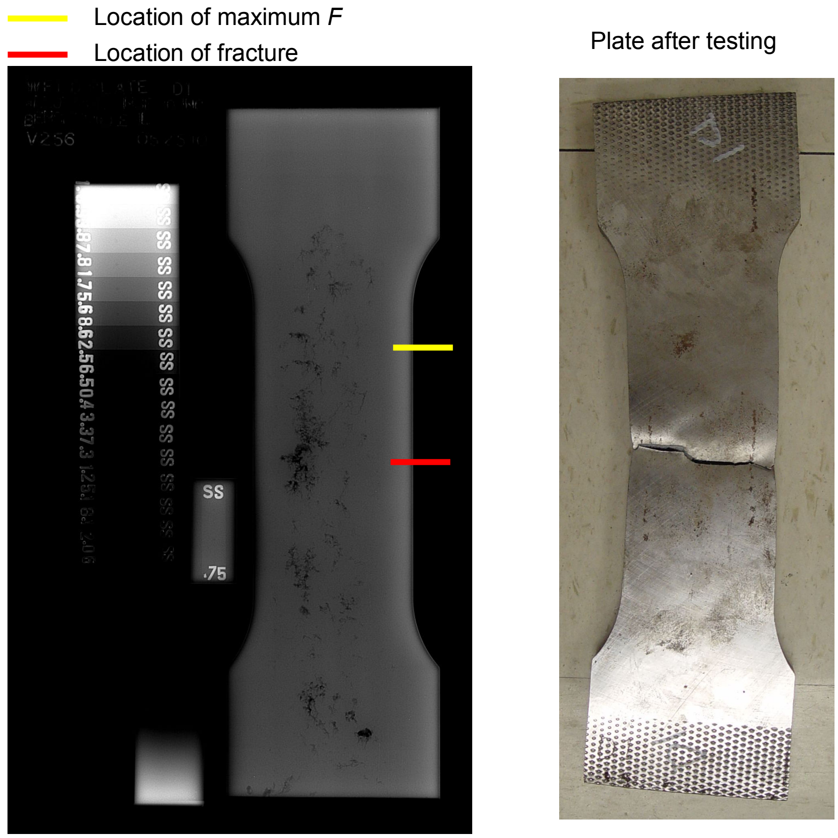

Figure 8. Radiograph and plate after testing for test plate D1 showing location of F and fracture.

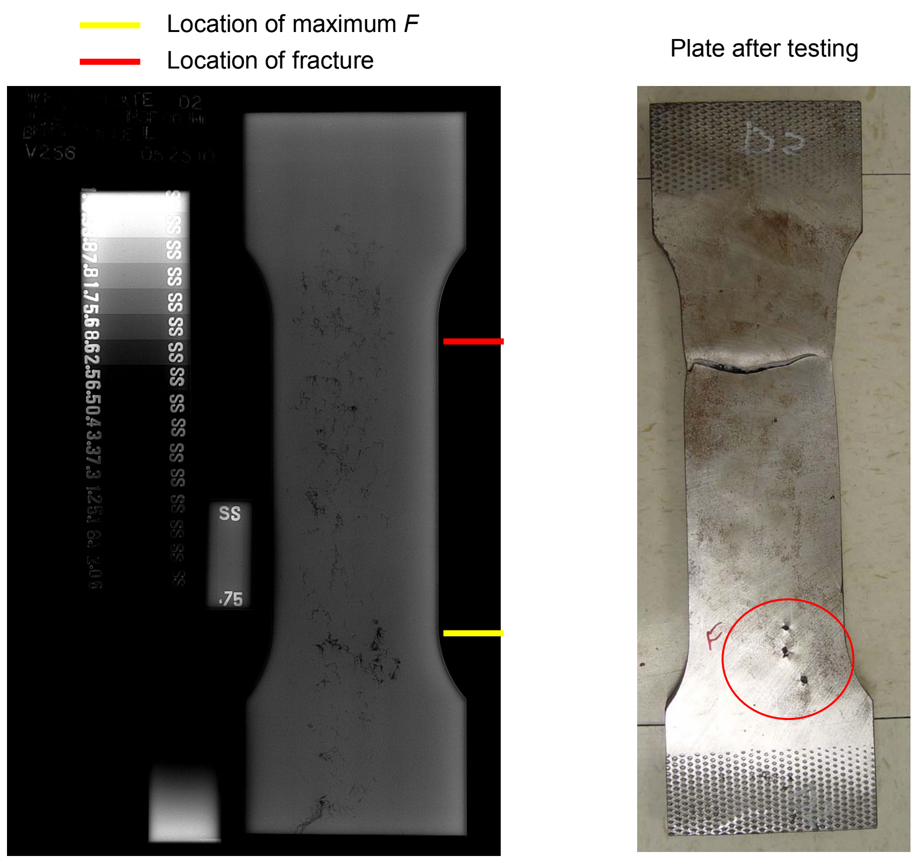

Figure 9. Radiograph and plate after testing for test plate D2 showing location of F and fracture.

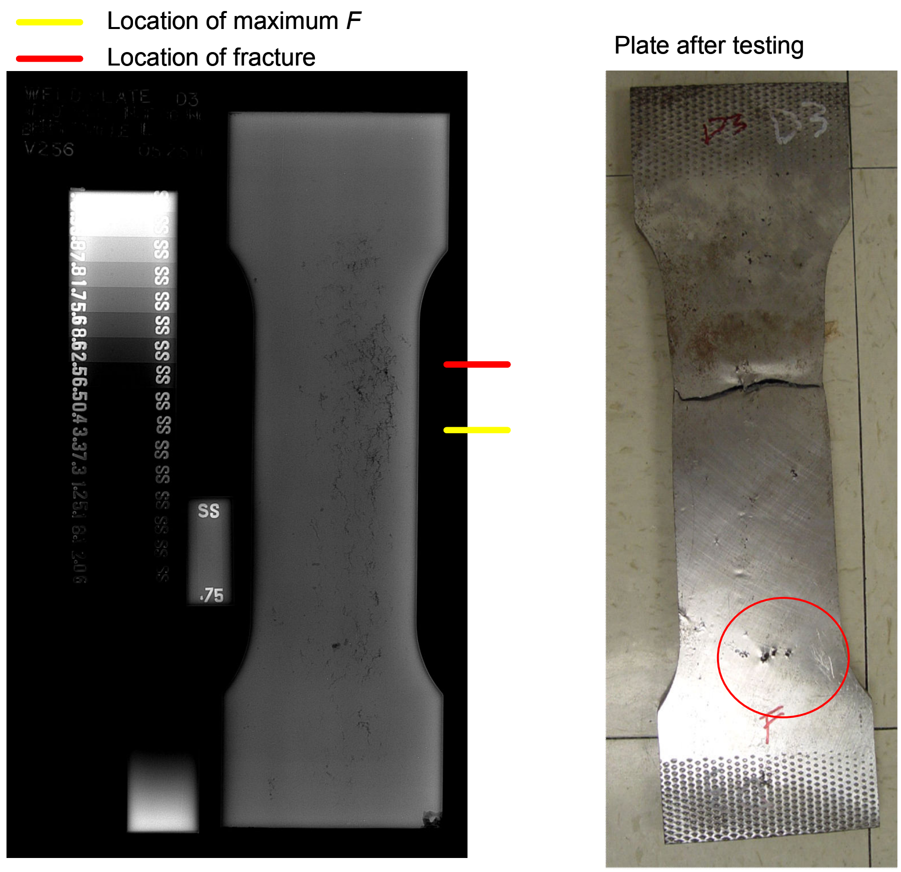

Figure 10. Radiograph and plate after testing for plate D3 showing location of *F* and fracture.

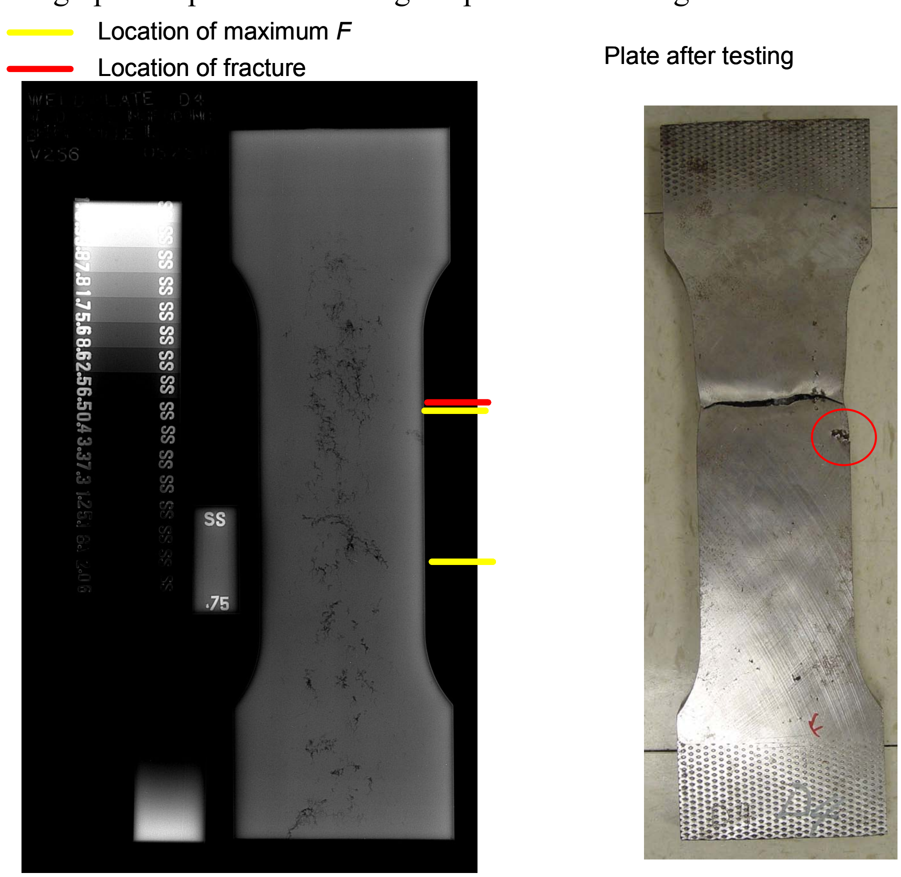

Figure 11. Radiograph and plate after testing for plate D4 showing location of *F* and fracture.

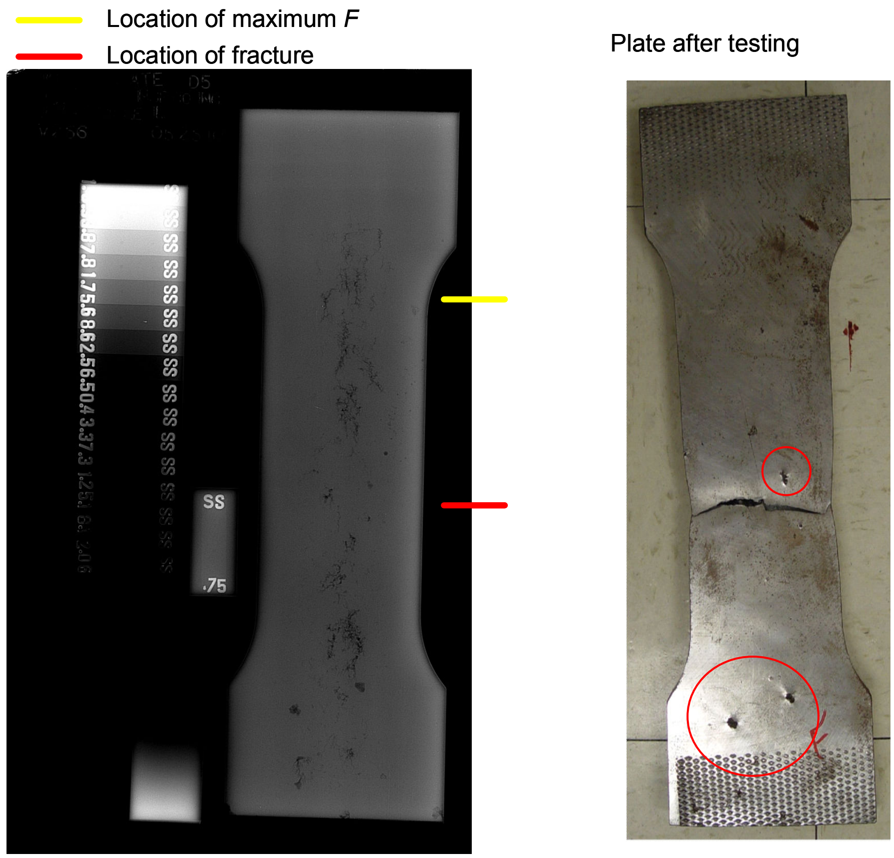

Figure 12. Radiograph and plate after testing for test plate D5 showing location of *F* and fracture.

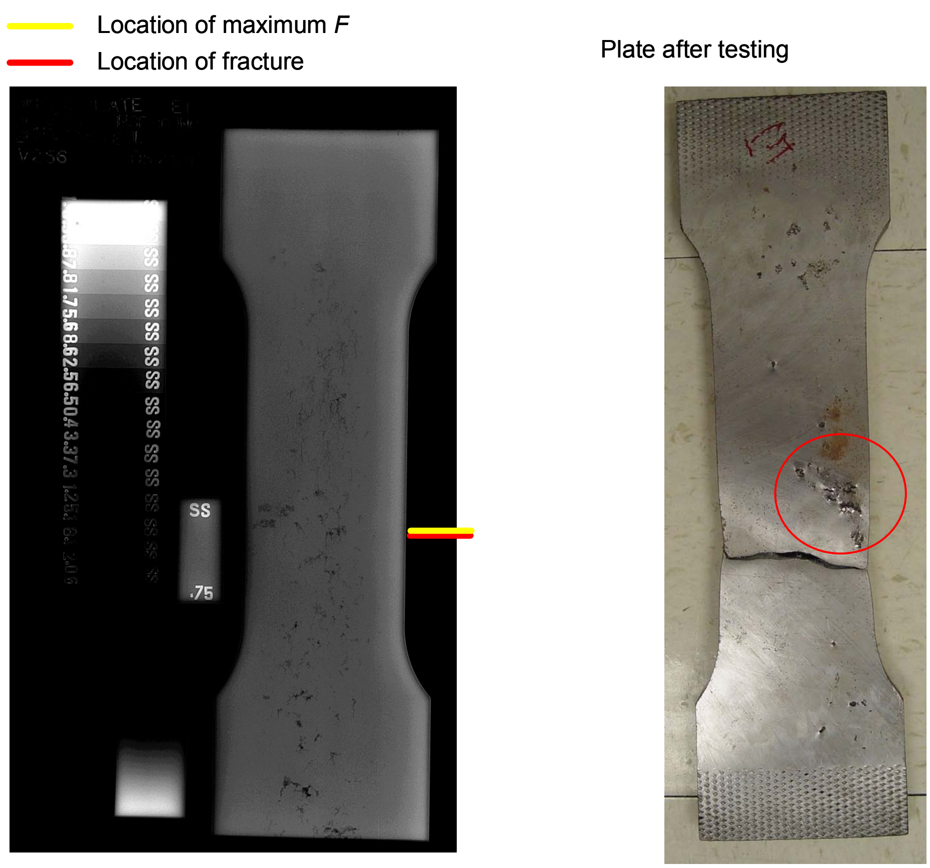

Figure 13. Radiograph and plate after testing for test plate E1 showing location of *F* and fracture.

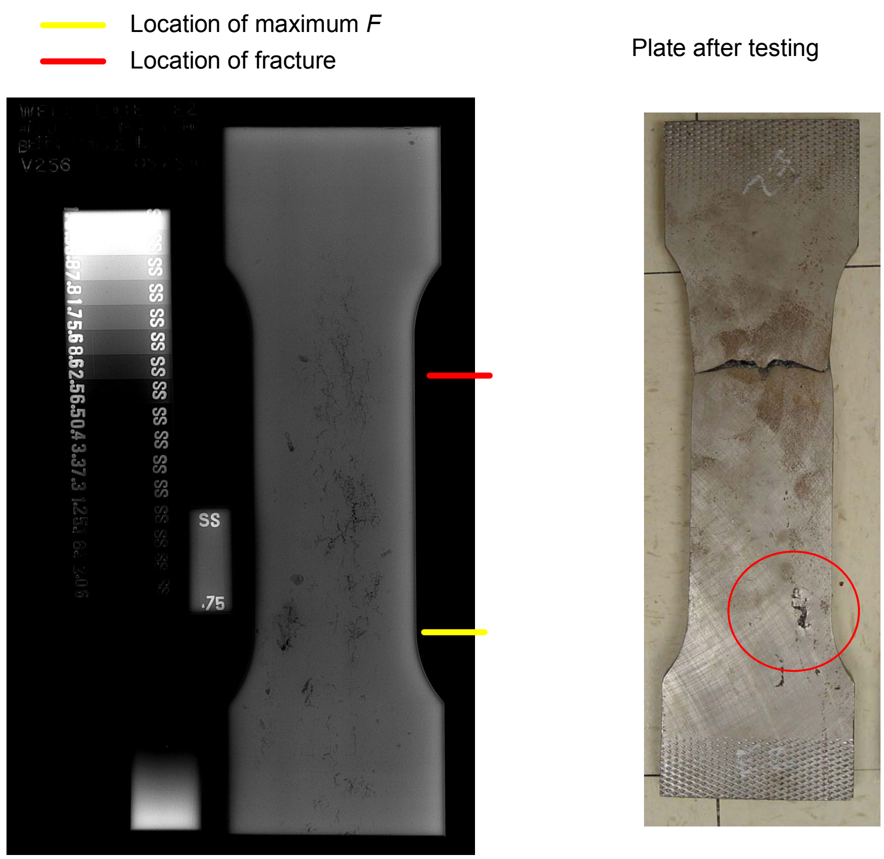

Figure 14. Radiograph and plate after testing for test plate E2 showing location of *F* and fracture.

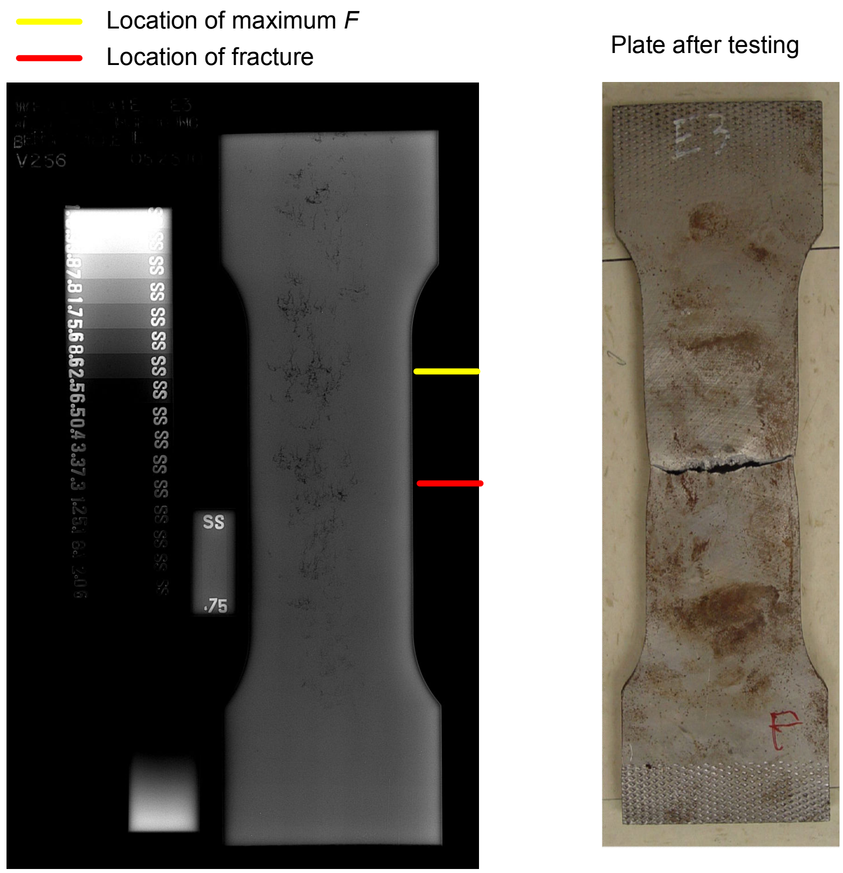

Figure 15. Radiograph and plate after testing for test plate E3 showing location of *F* and fracture.

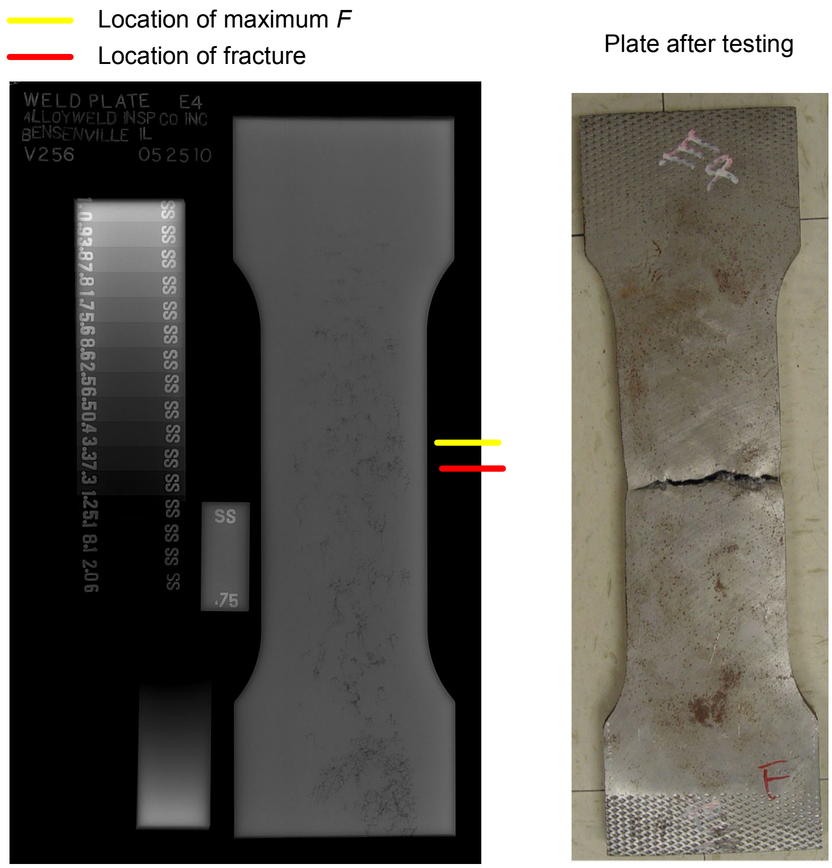

Figure 16. Radiograph and plate after testing for plate E4 showing location of *F* and fracture.

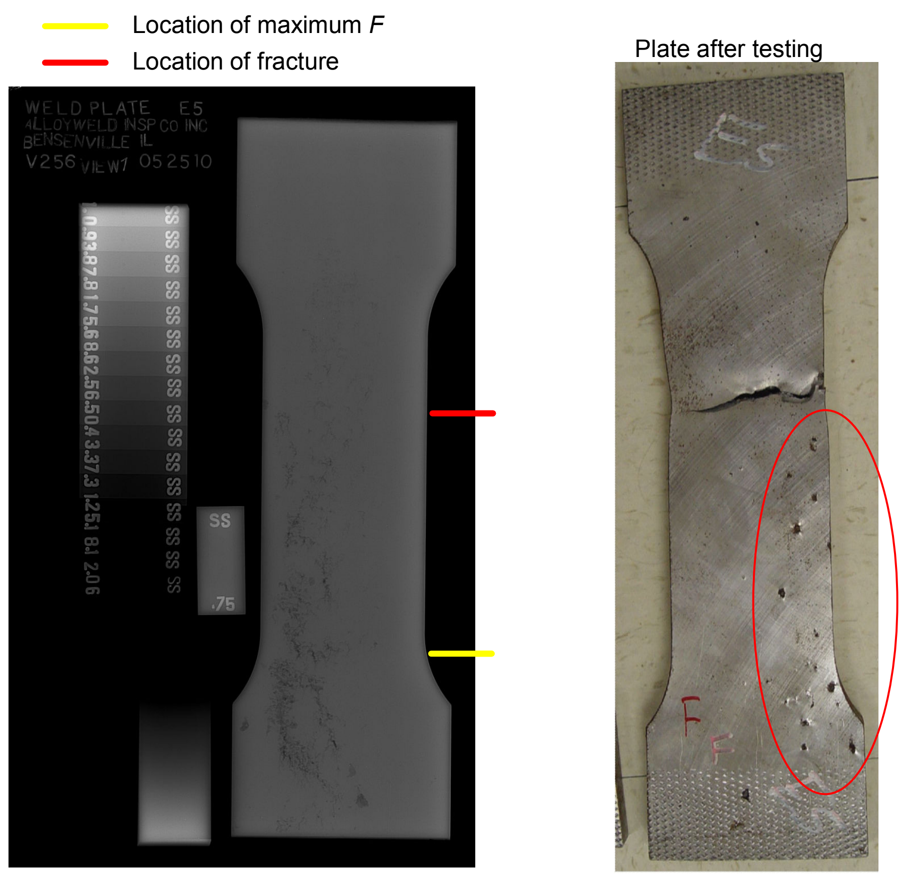

Figure 17. Radiograph and plate after testing for plate E5 showing location of *F* and fracture.

and a number ID, labeled plate D1 to D5 and E1 to E5, for a total of ten plates. All plates were vertically cast with a 1" thick by 5" wide cross section. All plates were top risered, and the letters D and E indicate two plate lengths. The D plates were 15" long, and the E plates were 18" long. It might be expected that the E family of plates have more porosity, since the feeding length is longer. In each radiograph in Figures 8 through 17 the location of the maximum indication fraction *F* along the plate length is given by the position of the yellow line. Figure 11 has the only radiograph with two yellow lines, indicating this was the only plate where the radiograph evaluators disagreed on the locations of *F*. The position of the fracture (which can also be gathered from the photo taken after testing) is indicated on each radiograph by a red line. Since the location of the failure can only be predicted by knowledge of the actual porosity distribution inside the plate, it is not surprising that the location of *F* and failure do not often coincide. The porosity distribution in the plates is dependent on the density of indications, or grey level, and that is not taken into account when determining *F*. Still the locations of *F* and failure coincide for plates D4, E1 and E4, Figures 11, 13 and 16, respectively. In a number of the photos of the plates after testing, substantial damage is observed at locations other than the final failure region. Some of these localized failure regions are circled in red, and clearly correspond to area with more indications on the radiographs.

The maximum indication fraction *F* for the ten tensile test plates determined by the new revised radiographic standard is shown in Figure 18. In Figure 18 the error bars signify the *F* values measured by the two radiograph evaluators. The largest F measured was about 60% (plate E4) and the smallest about 30% (plate D5). Note that all ratings of the plates except one, plate D5, fall into the Level 5 acceptance level indicated in Figure 4.

Stress-strain test curves for the sound specimen and the ten plates with porosity are shown in

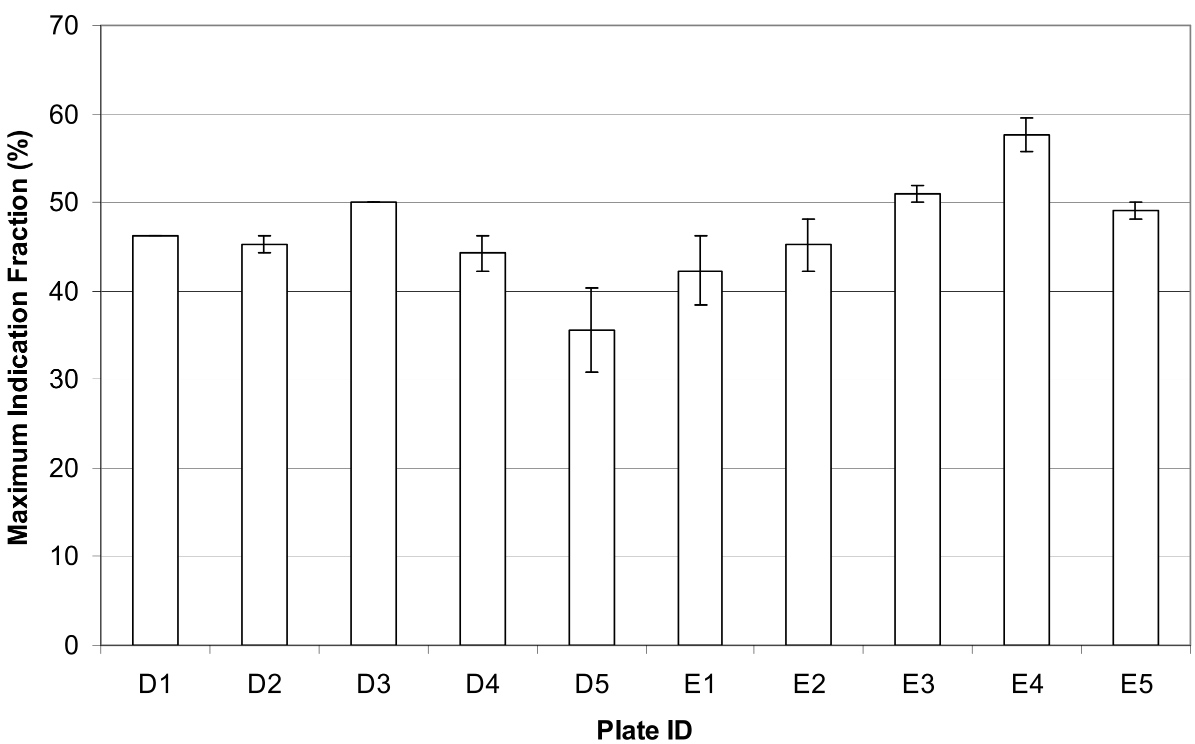

Figure 18. Results of rating film radiographs of tensile test plates using new RT standard.

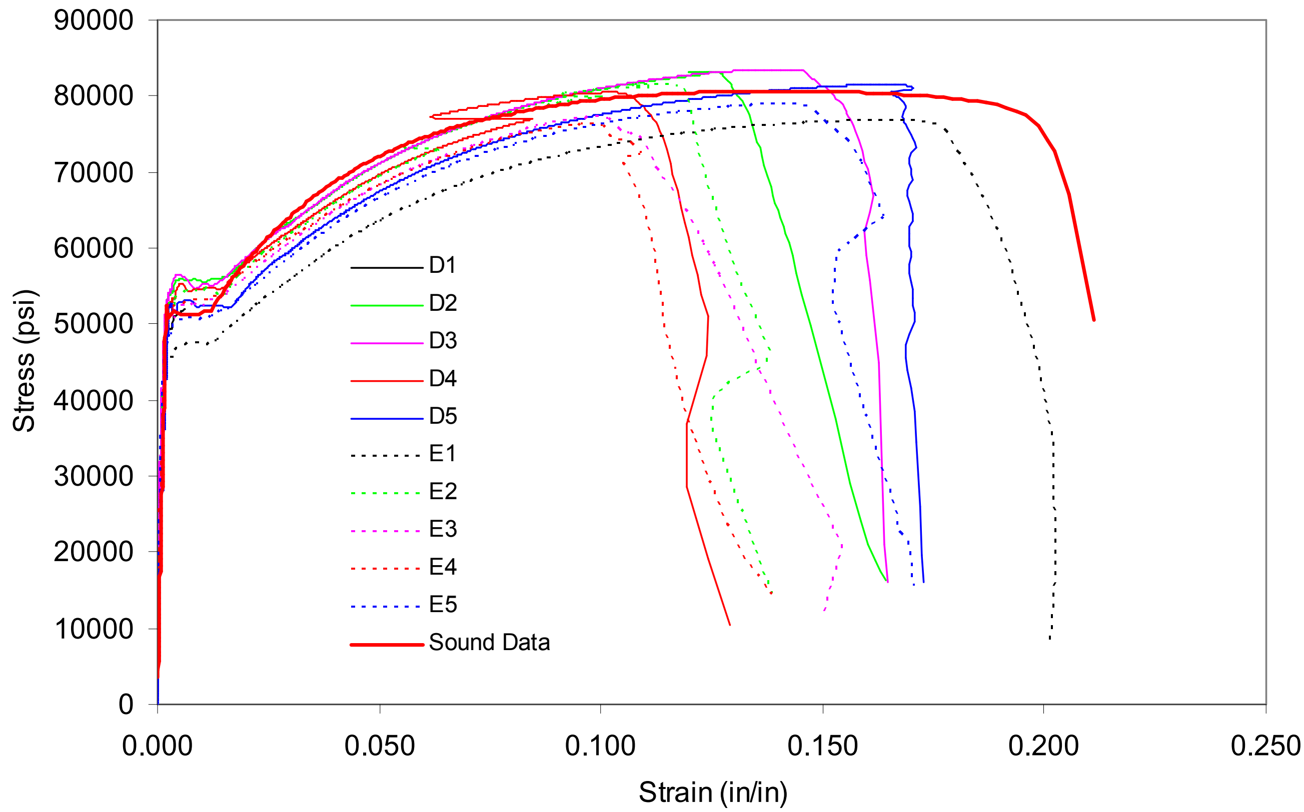

Figure 19. Full tensile testing stress-strain curves.

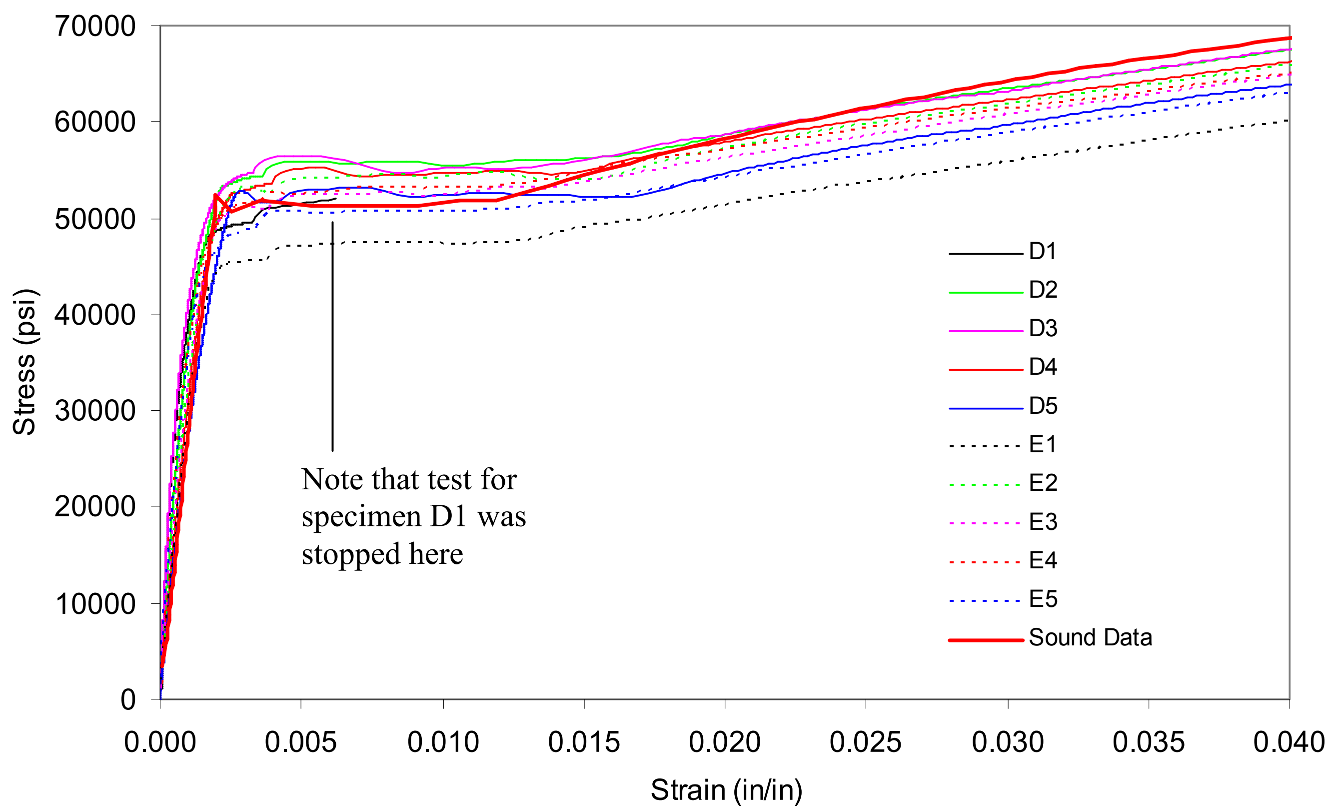

Figure 20. Stress-strain curves showing yield and plastic portions up to 0.04 strain.

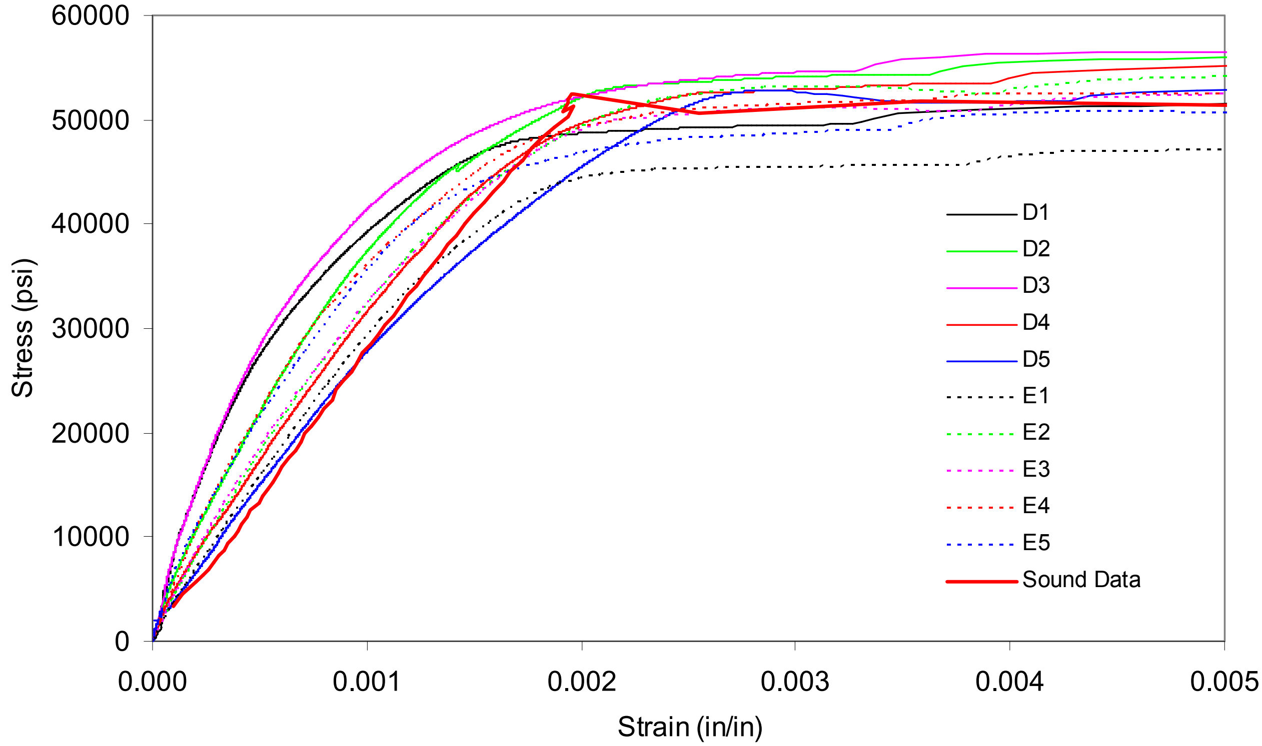

Figure 21. Lower strain region of stress-strain curves, up to 0.005 strain.

Figures 19 to 21. In Figure 19 the full tensile test curves are given, in Figure 20 the curves up to 0.04 strain are shown, and in Figure 21 up to 0.005 strain is shown to focus on the elastic range and yield points. The sound specimen test data was found to agree well with the standard ASTM A216 WCB properties: elastic modulus E_0 is 27,968 ksi (193 GPa), yield strength σ_{y0} is 52.4 ksi (361 MPa), ultimate tensile strength 80.6 ksi (556 MPa), and the elongation at fracture is 22%. These sound material properties for elastic modulus, yield strength, ultimate tensile strength (UTS) and elongation at fracture are plotted and compared to the those from the ten plates with porosity in Figures 22 through 25, respectively. The property values for the ten plates with porosity are given in Table 2. Unfortunately in the testing of specimen D1, the UTS and percent elongation were not acquired due to the machine automatically shutting down from an incorrect controller setting. The stopping point of the stress-strain curve for D1 is indicated in Figure 20.

Looking at elastic modulus results, note in Figure 21 that the elastic portion of the curve is clearly more linear for the sound data than for any of the porosity data. This nonlinearity in the plates with porosity is caused by local yielding and that regions within the plate are non-uniformly bearing the stress. It was difficult to determine the elastic modulus for the material with porosity because of the nonlinearity. Because of this, the elastic modulus for the porosity data was determined using a chord modulus between the stress-strain data at 10% and 90% of the yield stress [8]. As seen in Figure 22, the stiffness of the plates with porosity is clearly reduced from the sound data in each plate tested. If one were to rank the test plates by stiffness, four of the five highest measured elastic modulus plates are from the D family of plates, which should in theory be sounder than the E plates due to a shorter feeding distance when they were cast.

In Figures 20 and 23, note that the yield strength of the sound material is somewhat below the average of the test plates with porosity. Also in these figures, note that the "D" specimen plates

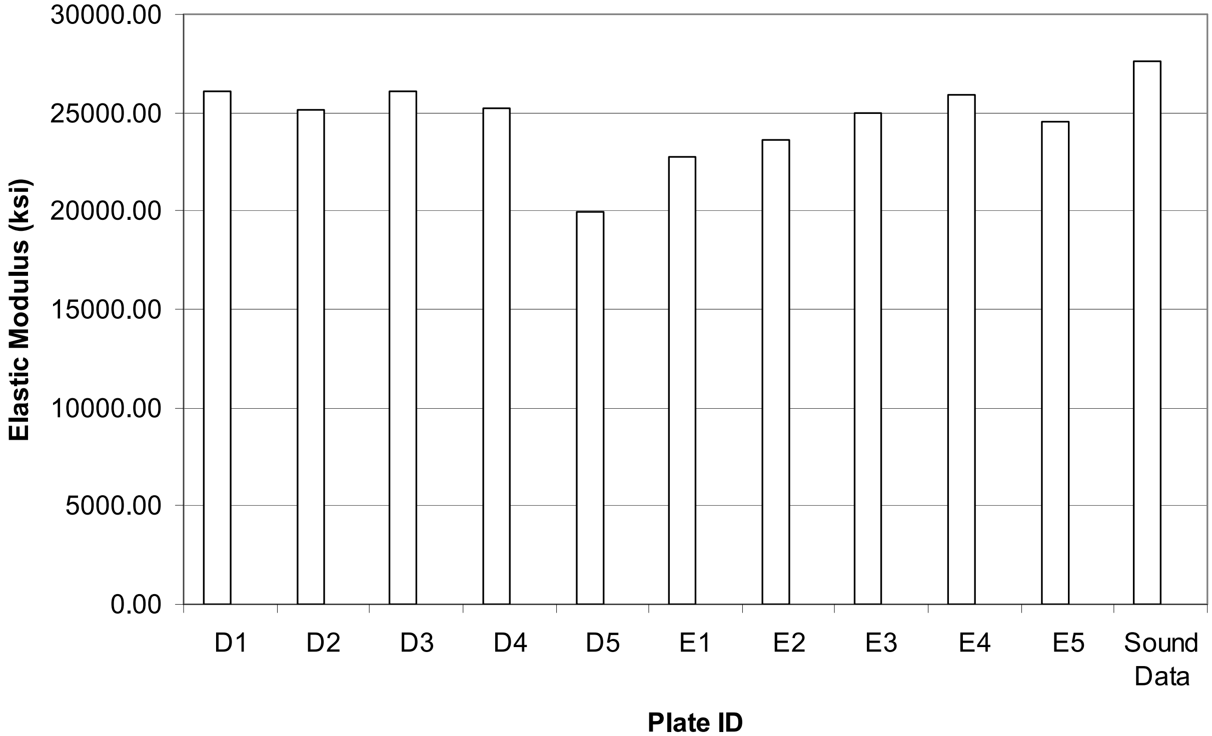

Figure 22. Elastic modulus from tensile testing of plates with porosity compared with sound data.

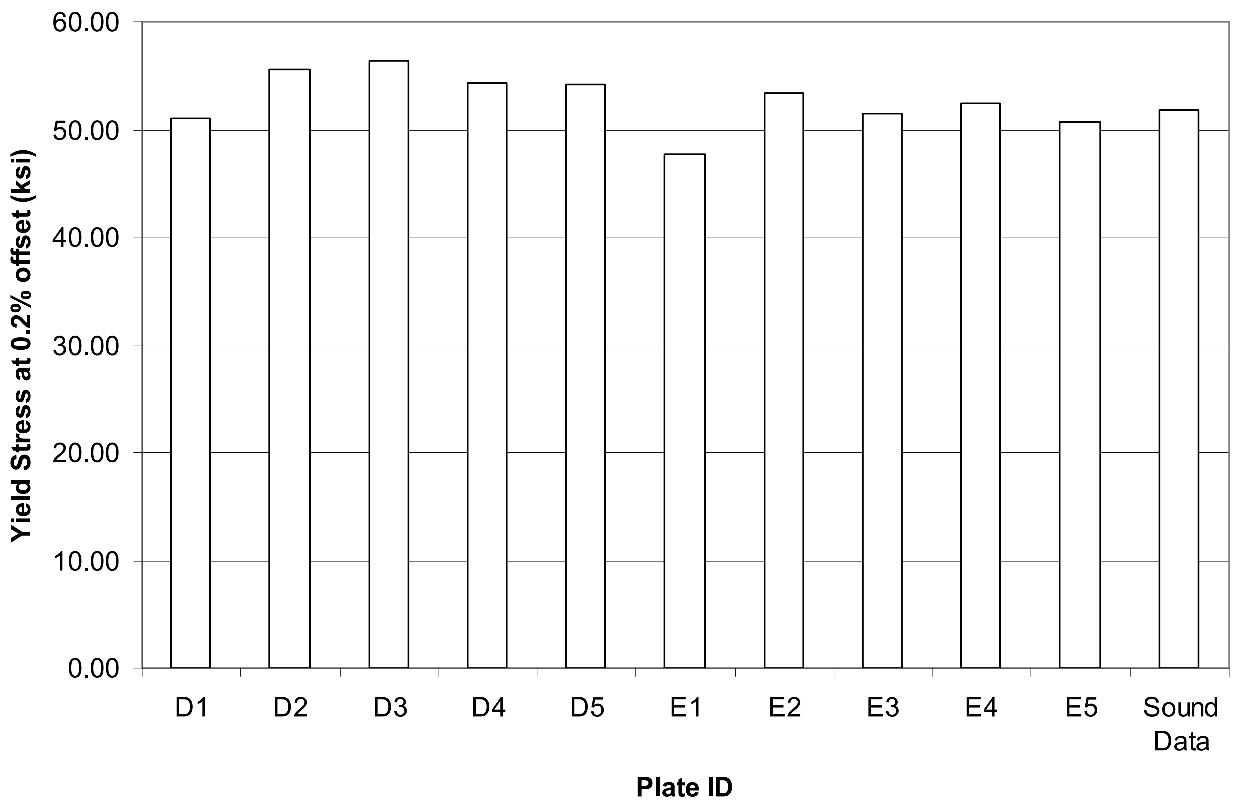

Figure 23. Yield stress (0.2% offset) from tensile testing of plates with porosity compared with sound data.

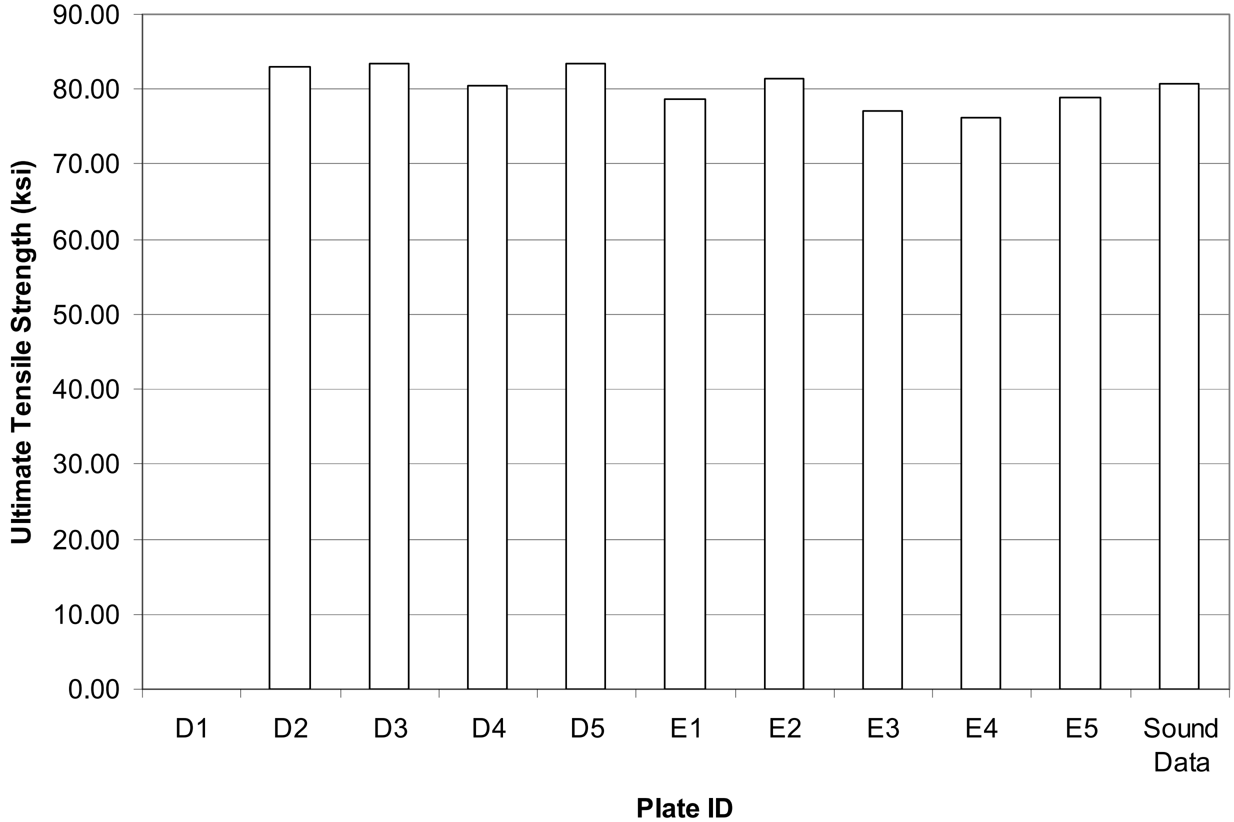

Figure 24. Ultimate tensile strength from testing of plates with porosity compared with sound data.

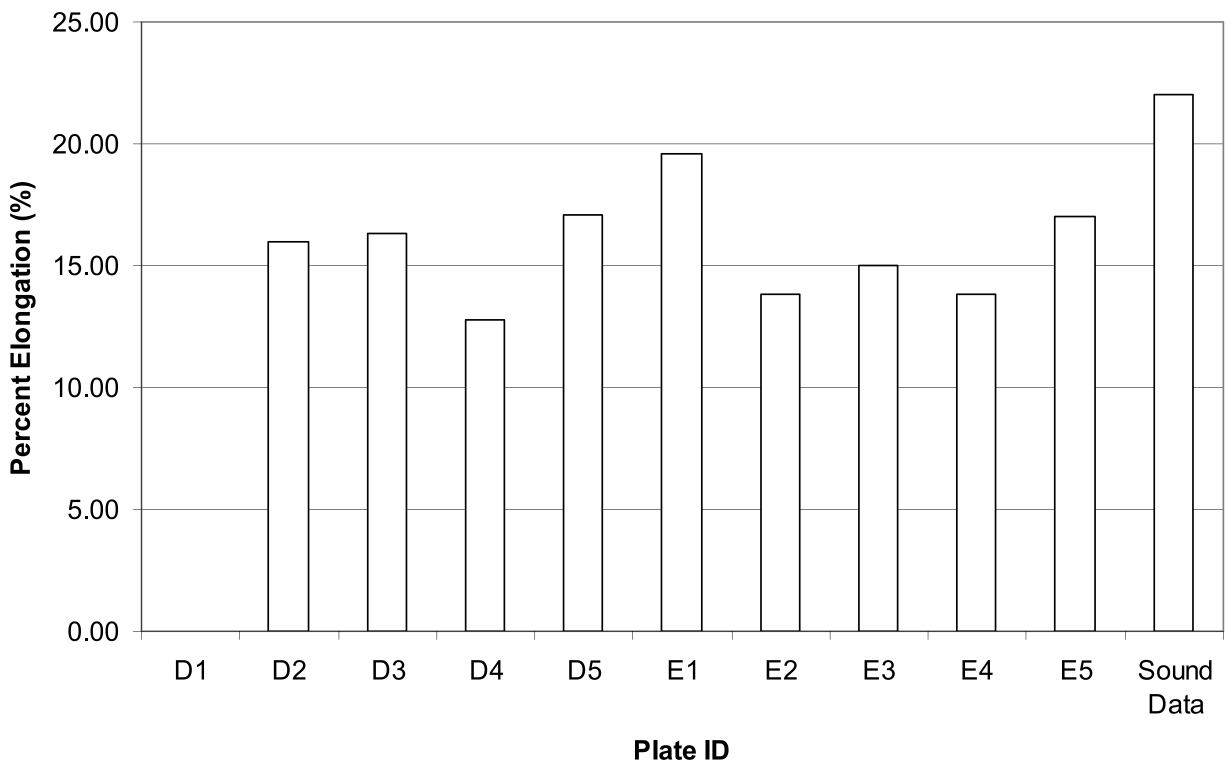

Figure 25. Percent elongation from tensile testing of plates with porosity compared with sound data.

Table 2. Tensile property measurements for tensile plates with porosity and sound datat.

Plate ID	Max. Ind. Fraction (%)	Elastic Modulus (ksi)	Yield Stress 0.2% (ksi)	UTS (ksi)	Elongation (%)
D1	46.15	26096	51.01	NA	NA
D2	45.19	25109	55.65	83.05	16.00
D3	50.00	26055	56.35	83.49	16.30
D4	44.23	25260	54.39	80.41	12.80
D5	35.58	19907	54.15	83.51	17.10
E1	42.31	22796	47.75	78.61	19.60
E2	45.19	23586	53.38	81.52	13.80
E3	50.96	24971	51.53	77.17	15.00
E4	57.69	25927	52.52	76.24	13.80
E5	49.04	24518	50.65	78.88	17.00
Sound Data	NA	27600	51.76	80.65	22.00

appear to have generally higher yield strengths than the “E” plates. Referring to Figure 18, the “E” plates were found to have slightly larger *F* measurements as well. Just as with stiffness, if one were to rank the test plates by yield strength, four of the five highest measured yield stress plates are from the D family of plates, which had a shorter feeding distance when they were cast. The yield stresses range from 48 to 56 ksi, and all would meet the minimum yield stress requirement for WCB steel (36 ksi).

In Figures 19 and 24 the ultimate strength of the sound material is among the highest values measured, but not the highest with 80.7 ksi. The range of all UTS data is from 76.2 to 83.5 ksi, and all data meet the UTS tensile requirement for WCB steel (70 to 95 ksi). Again, as with stiffness and yield strength, ranking the test plates by UTS one sees that four of the five highest measured UTS plates are from the D family of plates.

The sound material clearly has the greatest ductility with 22% elongation to failure (EL%) as shown in Table 2. Examining the stress-strain curves from Figures 19, and Figure 25, one sees that the plates with porosity have EL% values from 13% to nearly 20%, but the plate with ≈20% elongation might be an outlier. The reduction in ductility observed in the plates with porosity is perhaps the most obvious effect of the porosity on the tensile properties as seen in Figure 19.

The results of this tensile testing are compared to the proposed relationship between effective mechanical properties and the maximum radiographic indication fraction *F* shown earlier in Figure 4. To do this, the elastic modulus and yield stress properties of the ten test plates with porosity are normalized by their sound values, E_0 and σ_{y0}. The resulting values, the effective stiffness ratio E/E_0 and effective yield stress ratio σ_y/σ_{y0}, are given in Table 3. The effective stiffness ratio ranges between 0.72 to 0.95 for the plates with porosity, and the yield stress ratio was from 0.92 to 1.09. In Figures 26 and 27 the effective stiffness and yield stress ratio data are plotted versus the maximum indication fraction and compared with the proposed relationship between effective mechanical properties and the maximum radiographic indication fraction, *F*. The error bars in *F* denote the range of ratings made in the RT evaluation by the two raters.

Table 3. Property ratios (unsound/sound) for unsound plates and maximum indication fraction F ratings.

Plate ID	Max. Ind. Fraction (%)	Stiffness Ratio E/E_0	Yield Stress Ratio σ_y/σ_{y0}
D1	46.15	0.95	0.99
D2	45.19	0.91	1.08
D3	50.00	0.94	1.09
D4	44.23	0.92	1.05
D5	35.58	0.72	1.05
E1	42.31	0.83	0.92
E2	45.19	0.85	1.03
E3	50.96	0.90	1.00
E4	57.69	0.94	1.01
E5	49.04	0.89	0.98

It is clear that in both plots, the proposed relationship between mechanical properties and radiographic rating is conservative. Recall that the proposed relationship is based on the conservative assumption that any radiographic indication is a void through the entire plate thickness. The average stiffness ratio is 88% and the average maximum indication fraction is 48% (i.e. a typical level 5 plate). This means for the typical level 5 rated plate the designer can conservatively assume that they have at least 50% of the stiffness, when they actually have more. The yield stress property data show this proposed relationship to be even more conservative, since the average yield stress ratio is 102%. The designer can safely assume they have 50% of the yield stress properties. Again, the proposed relationship tested here (from Figure 4) results

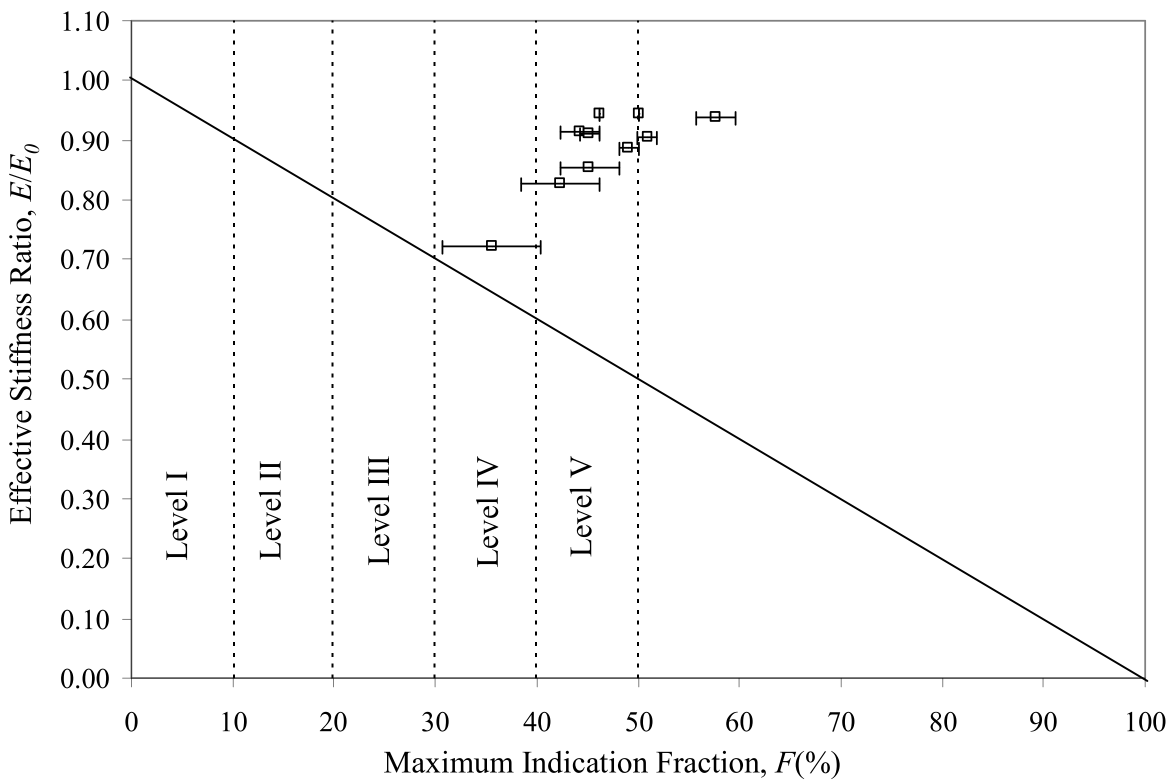

Figure 26. Effective stiffness ratio from tensile testing versus the maximum indication fraction data F compared with the proposed relationship between effective stiffness and the maximum indication fraction.

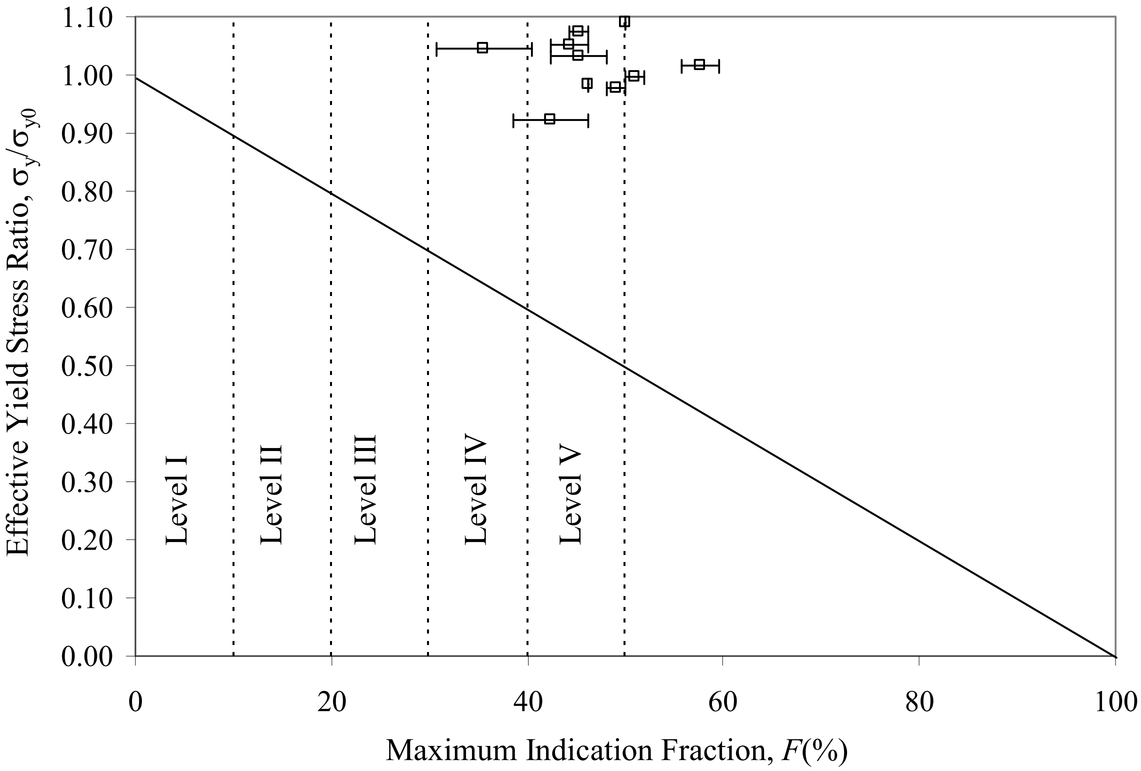

Figure 27. Effective yield stress ratio from tensile testing versus the maximum indication fraction data F compared with the proposed relationship between effective stiffness and the maximum indication fraction.

from the assumptions made (i.e. a plate in tension etc.). For other relationships between RT rating and performance, it would be up to designers to go through a similar exercise for their own assumptions and their own loading situation.

There were some observations made during the testing that should be documented. In two of the test plates, the strain data appeared to snap back to a lower value. The stress-strain data for the two plates (D4 and E2) with this “snap-back” behavior are shown in Figures 28 and 29, respectively. Since the initial positions of the knife edges on the plates were marked prior to testing, it could be determined if the extensometer slipped during and after testing. It could not be established that the extensometer slipped. From the handful of photos taken during testing of each of these plates (Figures 30 and 31), it is theorized that these snap-backs are cause by localized and significant failures in the plates that rapidly redistribute the stress and deformations throughout the plates. If one examines the data for plate D4 in Figure 28, the snap-back is about 2%, which for a 6” extensometer is a displacement of about 0.12”. It is conceivable that such a displacement could caused by a localized failure in the plate across from the extensometer, causing the extensometer side to bear more of the stress. This would cause the plate to bend in the width direction. To emphasize that this behavior is not a sudden slip of the extensometer, note in the zoomed-in data windows in both Figure 28 and 29 that when the snap-back occurs the data points show it to be a systematic event occurring over several data points in all cases. The data was stored every 10^{th} of a second during the testing. One can also see, with reference to Figures 30 and 31, that both plates deform more at some locations earlier in the testing than where the final failure occurs. As circled in Figure 30, for example, an area of porosity begins to open up, but as testing proceeds the final failure occurs in a different location. It should be noted

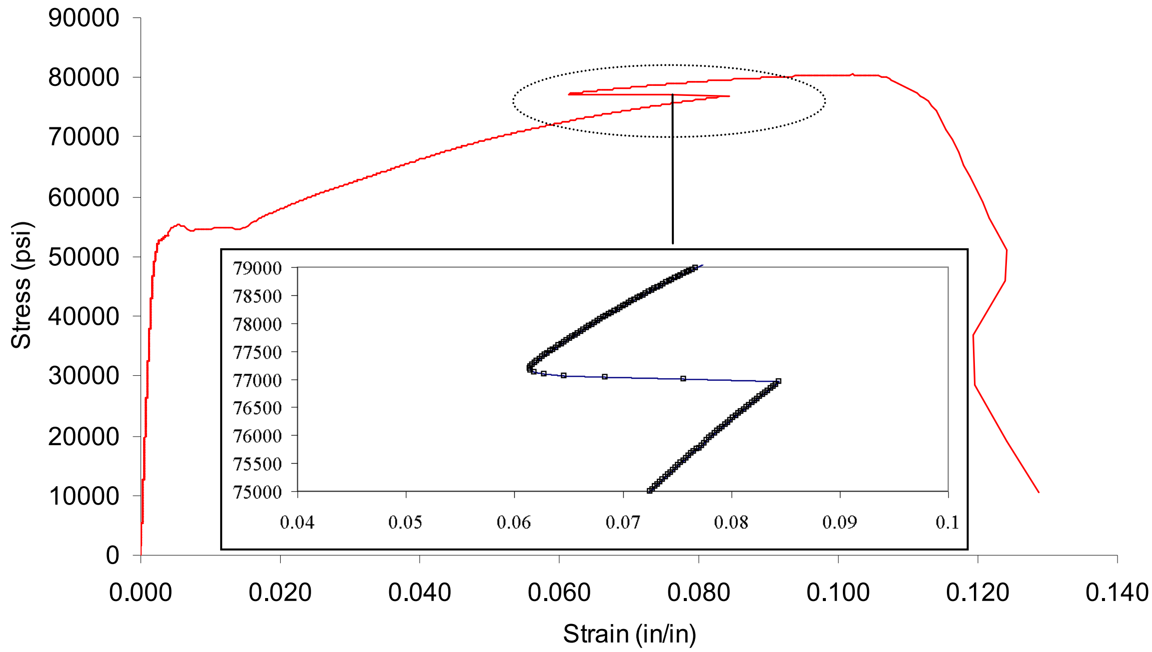

Figure 28. Stress-strain data for plate D4 showing the snap-back (circled) that was observed.

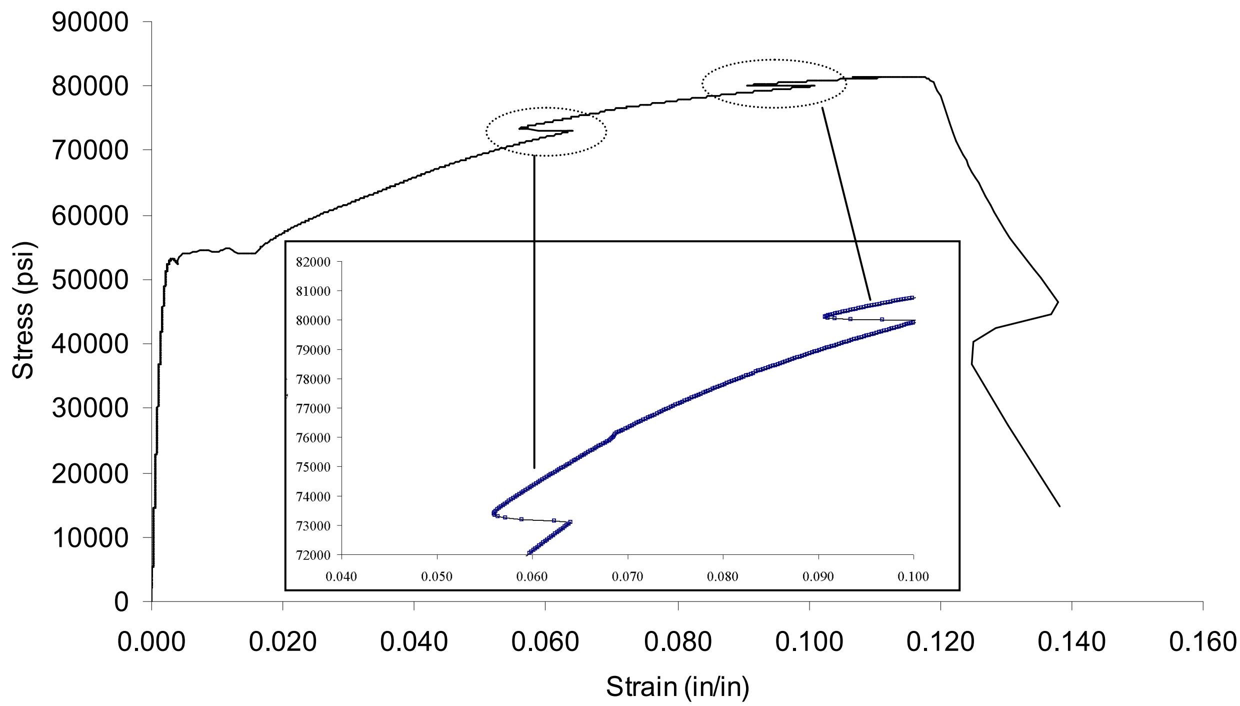

Figure 29. Stress-strain data for plate E2 showing the snap-back (circled) that was observed.

that "snap-forward" is difficult to determine from the data, because it appears (or would appear) to be the expected behavior of yielding and failing material data. Therefore, no clear determination of snap-forward can be made. The prediction of the rather complex failure of these plates could only be made by careful and accurate mapping of their porosity distribution into a finite element stress analysis that uses porosity dependent properties, damage and failure models.

Results Part II: Results of the Gage R&R Study of the Revised Radiographic Standard

The results of the gage R&R for the revised radiographic standard will now be presented. As mentioned earlier, three radiographs were rated by five readers three times each. The three radiographs used in the study were the same used in the 2009 gage R&R study. This way a fair comparison could be made between results for the earlier version and the revised version of the new RT standard. The three radiographs rated are given in Figures 32 to 34. Here the direction of interest (DOI) for the rating is the width of the radiograph.

The number of times a maximum indication fraction F was measured using the 0.25" wide ruler oriented in the DOI at a given position is given by the red numbers in Figures 32 to 34. Given that there are five RT "inspectors" with three evaluations each, there are at least fifteen Fs indicated in Figures 32 to 34. In some cases there are more fifteen, which means there was more than one location having the same F value in an inspector's measurement. Figure 33 has eighteen maximum indication fraction positions, and Figure 34, has sixteen F positions. The position with the largest number of agreements in F in Figures 32 and 33 are 5 and 4, respectively. In these two figures there is more scatter in the number of agreements about the position of F. In particular, radiograph #2 has eight different positions where F was measured; five times in four of these positions. Radiograph #2 (in Figure 33) was perhaps the most difficult to evaluate and measure. In contrast, radiograph #3 (in Figure 34) was perhaps the easiest to measure. Here for radiograph #3 there was one position which stood out in number of agreements on the measured F, with 11.

The mean indication fraction $\langle F \rangle$ is plotted in the left side white box histogram in Figure 35 for each radiograph, and the error bars give the interval for the total error from Table 4. The color histogram boxes in Figure 35 denote the mean ratings made by the individual radiograph evaluators and the error bars there denote the individual's confidence interval. The analogous plot from last year's gage R&R is shown in Figure 36, where there were seven evaluators in the study. The number in each histogram box denotes a different evaluator. Note that evaluator numbers in the two plots do not coincide to the same evaluator. In each radiograph the overall error is clearly reduced from last year's study, especially for radiograph #3. The revised standard appears to have properly addressed shortcomings in the earlier version of the new standard.

In Table 4 are given the overall mean indication fractions $\langle F \rangle$, the reader-to-reader reproducibility error $U_{F,1}$, the error in $\langle F \rangle$ due to reader repeatability, $U_{F,2}$, and the total error for $\langle F \rangle$ which includes $U_{F,1}$, $U_{F,2}$ and the ruler resolution for each radiograph. Since the errors appear to increase with the value of $\langle F \rangle$, it is interesting to express the errors in terms of percentage of $\langle F \rangle$. The errors in terms of percentage of $\langle F \rangle$ are given in Table 5, where the total errors range between 10% and 15% of the $\langle F \rangle$ value. Returning to Table 4, note that for

Figure 30. Pictures of plate D4 taken during testing with strain increasing from left to right. White arrow indicates position of failure.

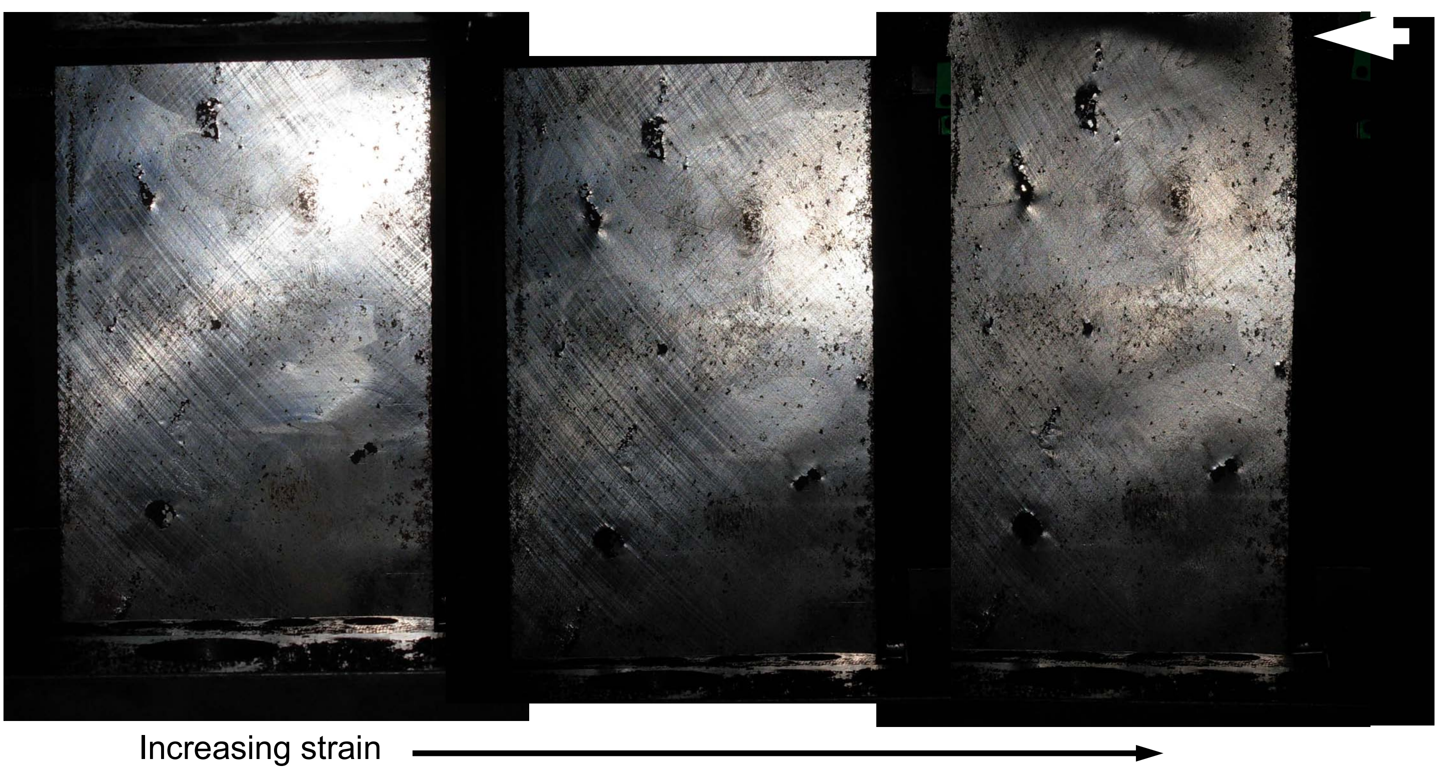

Figure 31. Pictures of plate E2 taken during testing with strain increasing from left to right. White arrow indicates position of failure.

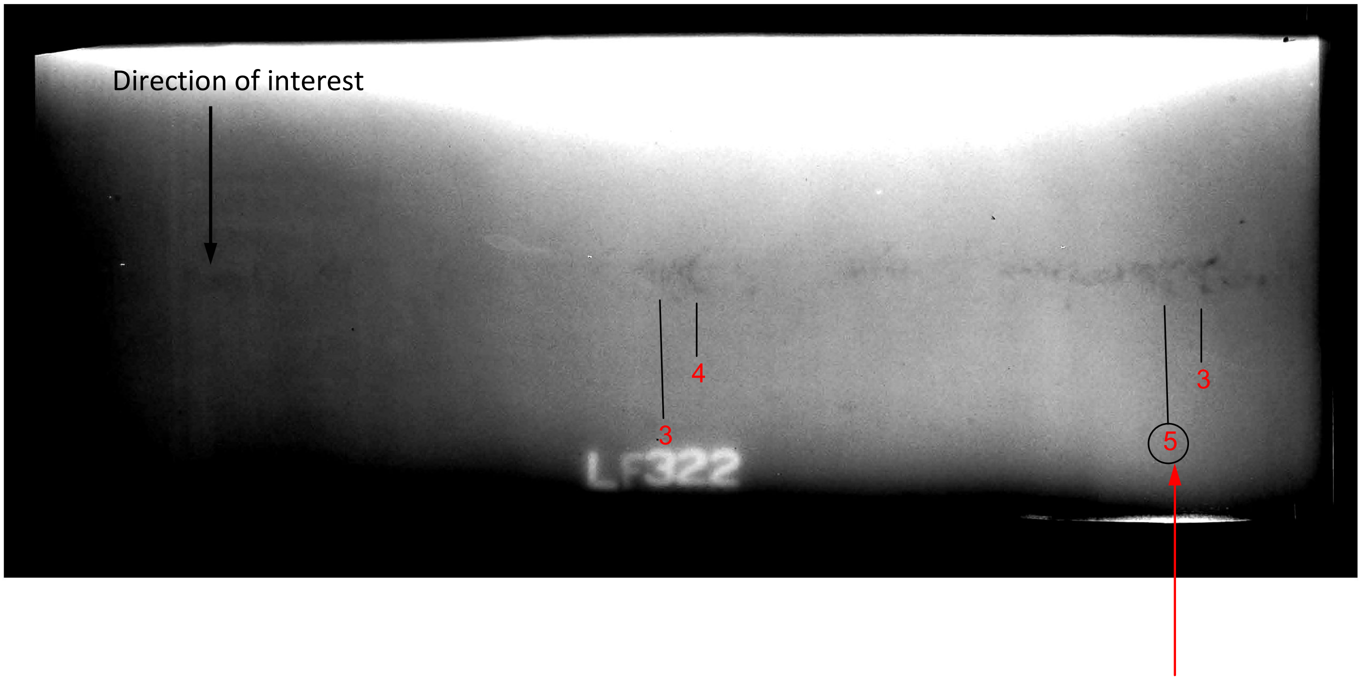

Figure 32. Radiograph #1 used in gage R&R study with locations of measured maximum indications and number of times that location was recorded at that location.

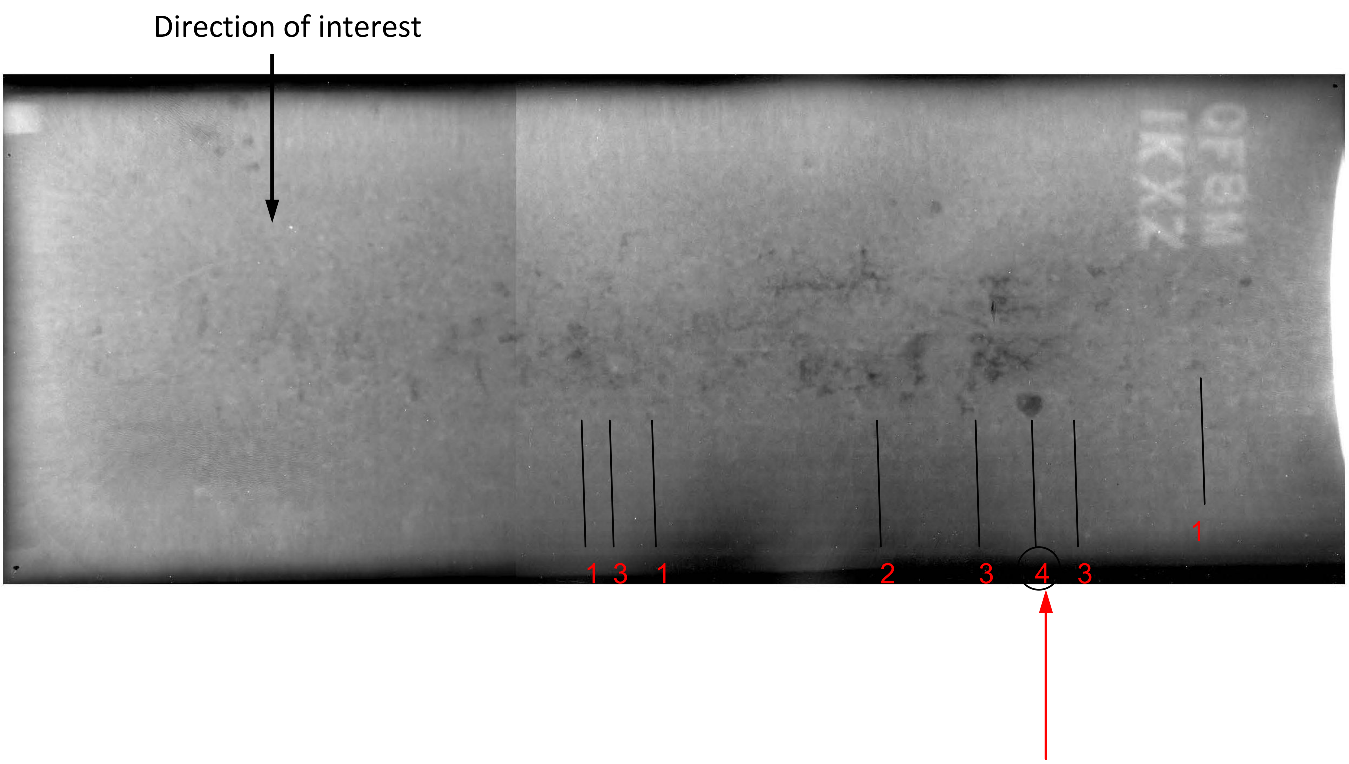

Figure 33. Radiograph #2 used in gage R&R study with locations of measured maximum indications and number of times that location was recorded at that location.

Figure 34. Radiograph #3 used in gage R&R study with locations of measured maximum indications and number of times that location was recorded at that location.

Table 4. Summary of Results from Gage R&R Study: Mean Indication Fractions and Errors

Radiograph ID	Overall Mean Indication Fraction, <F>	Error in <F> Due to Reader to Reader Variability and Bias, $U_{F,1}$	Error in <F> Due to Reader Repeatability, $U_{F,2}$	Total Error in <F>, RSS of $U_{F,1}$, $U_{F,2}$ and Ruler Resolution
X-Ray #1	0.1175	0.0134	0.0098	0.0177
X-Ray #2	0.3525	0.0339	0.0159	0.0380
X-Ray #3	0.1067	0.0086	0.0032	0.0111

Table 5. Summary of Results from Gage R&R Study: Mean Indication Fractions and Percent Errors of <F>

Radiograph ID	Overall Mean Indication Fraction, <F>	Error in <F> Due to Reader to Reader Variability and Bias, $U_{F,1}$ (%)	Error in <F> Due to Reader Repeatability, $U_{F,2}$, (%)	Total Error in <F>, RSS of $U_{F,1}$, $U_{F,2}$ and Ruler Resolution (%)
X-Ray #1	0.1175	11%	8%	15%
X-Ray #2	0.3525	10%	5%	11%
X-Ray #3	0.1067	8%	3%	10%

all radiographs in this gage R&R, the total error is less than ½ of a rating level of F (since a level of F is 0.1 and half a level is 0.05, and the largest error is 0.038). The largest source of error in this gage R&R study is the reader-to-reader reproducibility error $U_{F,1}$. This was also the case in the previous gage R&R [3], but here $U_{F,1}$ has been reduced by 35%, 32% and 70%, for radiographs #1, #2 and #3, respectively, from the previous gage R&R study. The error in $\langle F \rangle$ due to reader repeatability $U_{F,2}$ is either unchanged or greatly reduced from the previous study, where $U_{F,2}$ was 0.0073, 0.0319 and 0.0155 for radiographs #1, #2 and #3, respectively. In the current study $U_{F,2}$ was 0.0098, 0.0159 and 0.0032 for radiographs #1, #2 and #3, respectively. To visualize the reductions in the errors observed with use of the revised standard, compare the one-sided errors in $\langle F \rangle$ due to the reader-to-reader reproducibility and reader repeatability plotted for the three radiographs in Figure 37 for the current study with those in Figure 38 for the 2009 study. Here it is apparent that all errors are substantially reduced in the current study except for the repeatability error for x-ray #1, which is essentially unchanged as previously mentioned.

As is commonly done in gage R&R studies, analysis of variance (ANOVA) is used to test whether the proportion of the variation "between readers" to variation "within all readers" is statistically significant. Ideally one would like to eliminate the between-reader variation, so the operator is not relevant to the RT rating. However, the reader-to-reader error is the largest error, and it would be surprising if it was not statistically significant. The ANOVA results are given in Tables 6, 7 and 8 for radiographs #1, #2 and #3, respectively.

The entries in Table 6 to 8 are the sources of variation, the sum of the squares of the indication fraction variations for each source (*SS*), the degrees of freedom for each source (*df*), the mean square of the variation of each source (*MS*), the calculated F-statistic (*F-stat*) and the P-value, and the F-critical value for the significance level chosen and degrees of freedom. The level of significance chosen for this analysis is $\alpha = 0.05$. If the P-value resulting from the analysis is less than α, than the probability is small relative to α that the differences in variations between the readers and within the readers is random. If this occurs, the null hypothesis (that there is no systematic difference in the readers' measurements) is rejected and the differences between readers are statistically significant. An alternate, but equivalent, test is to compare the calculated F-statistic to the F-critical value. If the calculated F-statistic is greater than the critical F-statistic for the significance level and degrees of freedom, the differences between the readers is systematic (not random), and also leads us to reject the null hypothesis.

In Table 6 note that the calculated F-statistic (*F-stat*) is less than the critical F-statistic which indicates that the differences between the readers is random, and there is no systematic reader-to-reader variability. In Tables 7 and 8, for radiographs #2 and #3, this is not the case, and there are systematic differences between the readers' evaluations. However, in Tables 7 and 8 the *F-stat* values are not too much larger than the critical F-statistic. It can be shown that there is no systematic reader-to-reader variability if the ANOVA analysis were to be performed at the $\alpha = 0.039$ and 0.022 significance levels for the data for radiographs #2 and #3, respectively. Such tests are less stringent than the $\alpha = 0.05$ level of significance, but still point to a reduction in reader-to-reader variability over last years' results.

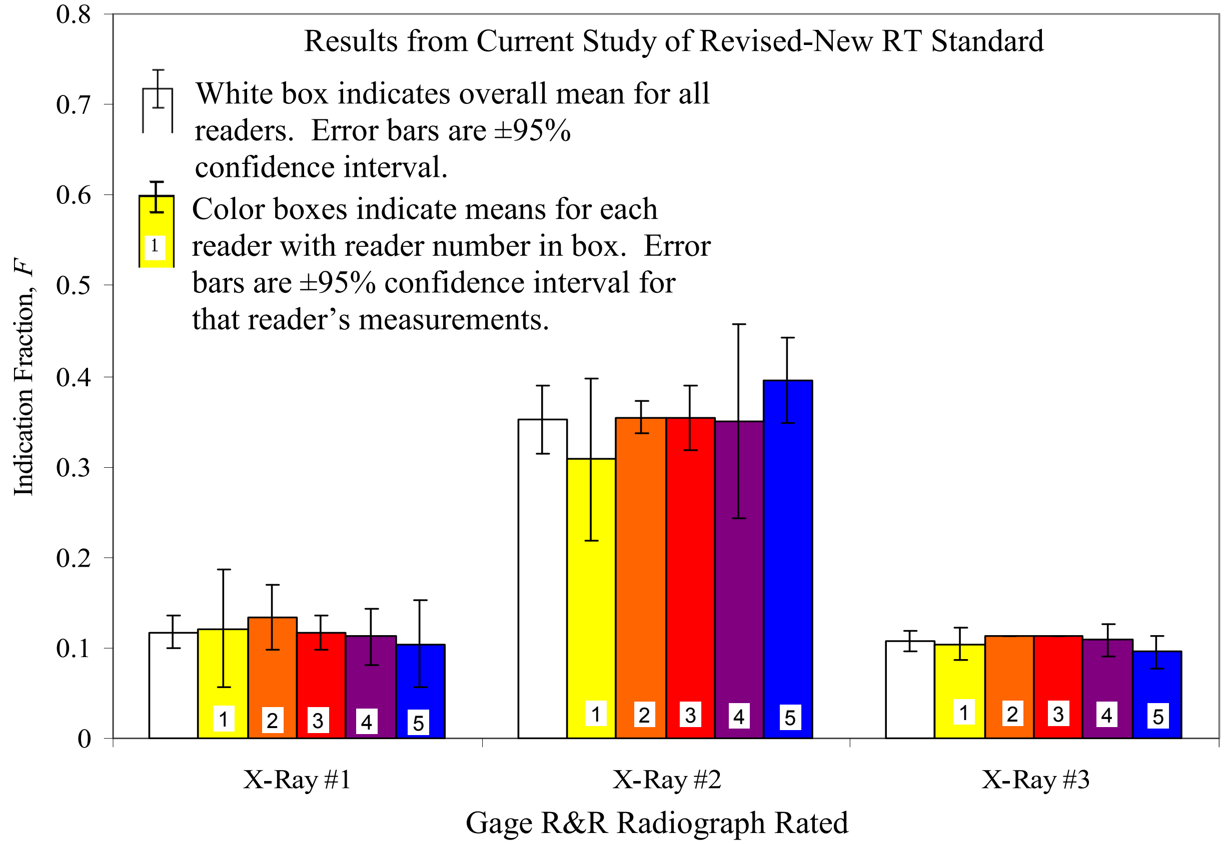

Figure 35. Mean indication fractions (overall, and by reader) and 95% confidence intervals from the current study.

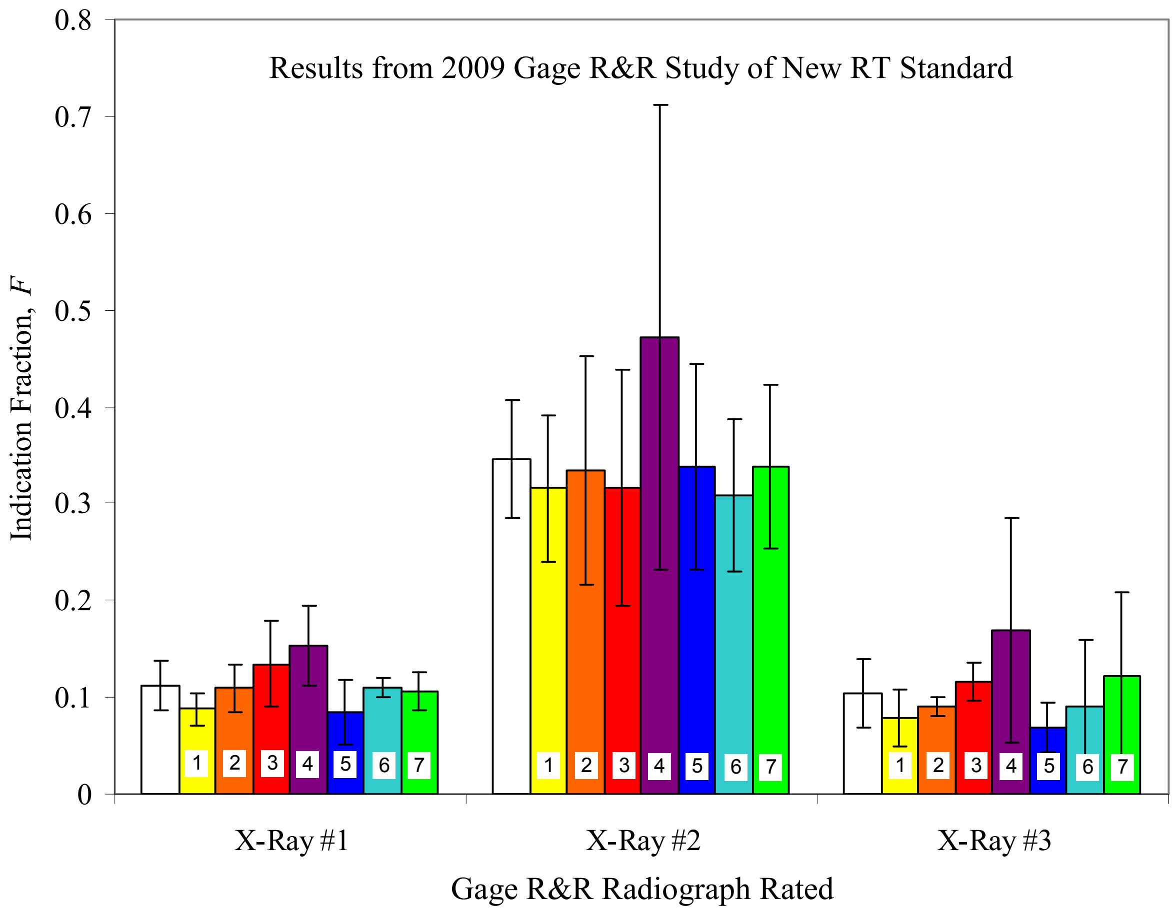

Figure 36. Mean indication fractions (overall, and by reader) and 95% confidence intervals from the 2009 study [3].

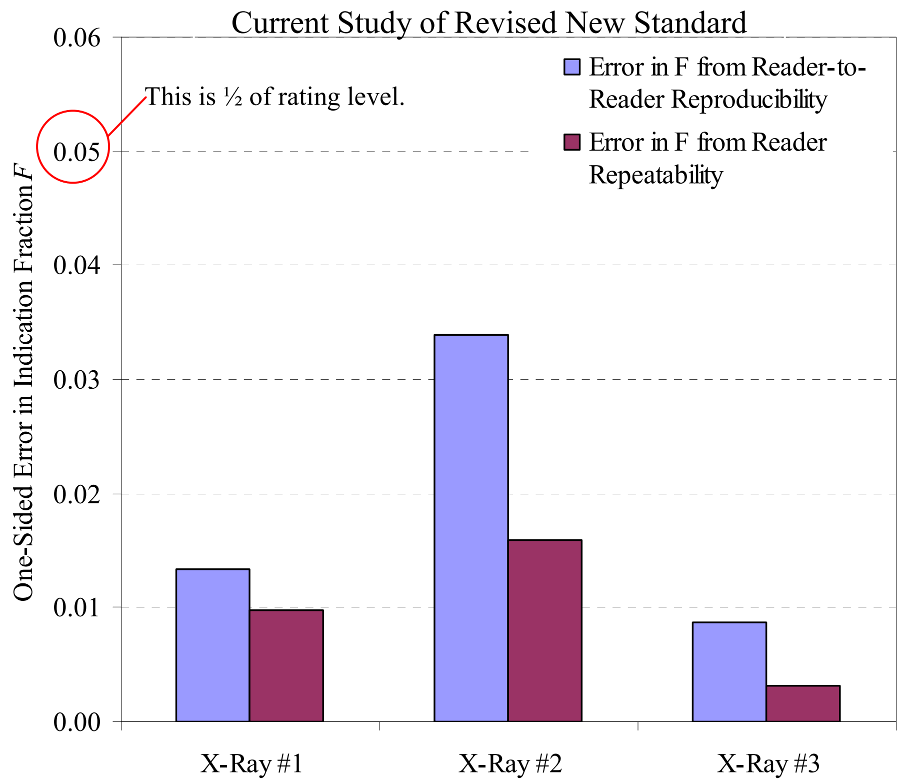

Figure 37. Reader reproducibility and repeatability errors determined from the current Gage R&R study

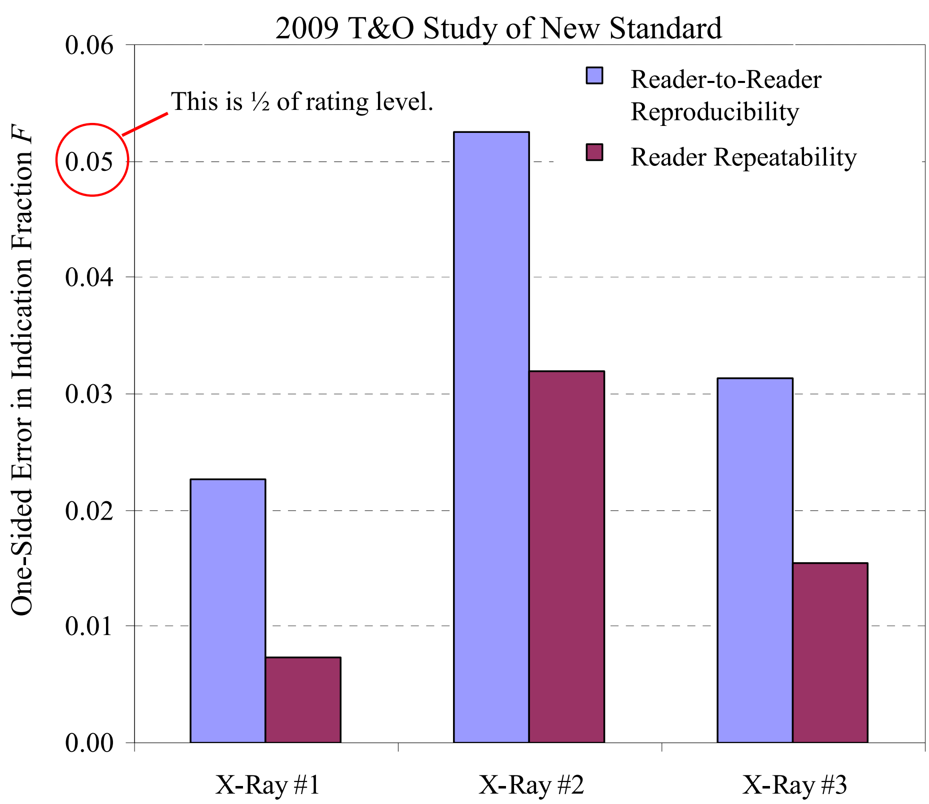

Figure 38. Reader reproducibility and repeatability errors determined from the 2009 Gage R&R study

Table 6. Analysis of Variance Results: One-way ANOVA table for Radiograph #1

Source of Variation	*SS*	*df*	*MS*	*F-stat*	*P-value*	*F-critical*
Between Readers	0.001395	4	0.000348	1.19642	0.37052	3.47804
Within All Readers	0.002916	10	0.000291			
Total	0.004312	14				

Table 7. Analysis of Variance Results: One-way ANOVA table for Radiograph #2

Source of Variation	*SS*	*df*	*MS*	*F*	*P-value*	*F-critical*
Between Readers	0.011520	4	0.002880	3.787671	0.039866	3.478049
Within All Readers	0.007604	10	0.000760			
Total	0.019125	14				

Table 8. Analysis of Variance Results: One-way ANOVA table for Radiograph #3

Source of Variation	*SS*	*df*	*MS*	*F*	*P-value*	*F-critical*
Between Readers	0.000583	4	0.000145	4.6666	0.021983	3.4780
Within All Readers	0.000312	10	0.000031			
Total	0.000895	14				

IV. CONCLUSIONS AND RECOMMENDATIONS

Part I: Validation of Relationship between RT Acceptance and Mechanical Performance

In the first study presented in the paper, a proposed relationship between RT acceptance criteria and mechanical performance of castings in tension was tested and validated. It was shown that 0.75" inch thick plate castings with large amounts of porosity, falling into the worst RT acceptance level (level 5), still retained 88% of their sound stiffness and all of their yield properties. The relationship between RT acceptance criteria and mechanical performance castings tested here conservatively recommends that the designer assumes the casting would have 50% of these properties for RT acceptance level 5. This relationship is based on assumptions about the radiographic indications for a given loading. It can serve as an example to designers in the development of other relationships for casting sections in tension or different loading conditions, which might be more or less conservative. As stated in the new RT standard, it is up to the designers who specify the RT acceptance criteria to relate it to mechanical performance.

During the testing of the plates, the snap-back behavior that was observed is thought to be related to localized failures and stress redistribution occurring as a result. If such testing were done in the future, a high quality video recording of the test is recommended, since it might be able to capture such events and clearly explain them.

The new RT standard cannot provide a prediction on the location and manner of the casting failure (i.e. damage and strain to failure). This is because it does not consider the grey level of indications on radiographs or provide a way to determine the porosity distribution in the casting. Only after reconstructing the porosity distributions in the plates based on their grey level, and mapping this porosity distribution into finite element stress analyses (FEA), and using porosity dependent properties, damage and failure models in the FEA, can the location and manner of the failure be predicted. While the authors recommend pursuing this to validate FEA models that consider the effects of porosity, the results from that work will not change the outcome of this work, a validated relationship between RT acceptance and mechanical performance.

Part II: Gage R&R Study of the Revised Radiographic Standard

When applying the new radiographic standard, measurements of the maximum indication fraction are made. There is variability in these measurements due to the individual making the measurements, the radiograph itself and how the measurements are made. The radiographic standard was revised to address shortcomings observed in an earlier gage R&R study. Here it was demonstrated that the revised standard gives lower reader-to-reader reproducibility and reader repeatability errors in the RT ratings. The largest source of error in the gage R&R study is the reader-to-reader reproducibility, but it was reduced by 46% on average compared to last years gage R&R study. The error due to reader repeatability was reduced by an average of 30% from the previous study. Compared to the current ASTM RT standards, which have been shown to have an average confidence interval of ±1.4 levels [2], the revised new RT standard gives confidence intervals of ±0.17, ±0.38, and ±0.11 levels for the three radiographs evaluated in the study. In last year's gage R&R study, the earlier version of the new RT standard gave confidence intervals of ±0.25, ±0.62, and ±0.36 levels for the same three radiographs. The new revised standard was also shown to reduce the between-readers variability in an AVOVA analysis. It is not expected that the to reader-to-reader variability be eliminated, but the reduction in reader-to-reader variability over last years' gage R&R results reflect the improvements made to the revised standard. It is recommended the standard be put forward to ASTM to serve as an additional radiographic testing standard that can be used to relate RT acceptance criteria to mechanical performance.

ACKNOWLEDGEMENTS

This research was undertaken through the American Metalcasting Consortium (AMC). AMC is sponsored by Defense Supply Center Philadelphia (DSC, Philadelphia, PA) and the Defense Logistics Agency (DLA, Ft. Belvoir, VA). This work was conducted under the auspices of the Steel Founders' Society of America (SFSA) through substantial in-kind support and guidance from SFSA member foundries. In particular, the authors gratefully appreciate the participation of Sivyer Steel Casting for heat treating the tensile test plates. The valuable tensile test data could not have been acquired without the 800,00 lb force capacity test machine at SSAB North American Division, Muscatine, Iowa. The authors thank SSAB, and Brian Castillo, their laboratory supervisor, for running the tensile tests.

Any opinions, findings, conclusions, or recommendations expressed herein are those of the authors and do not necessarily reflect the views of DSC, DLA, or the SFSA and any of its members.

REFERENCES

1. Blair, M., Monroe, R., Hardin, R.A., and Beckermann, C., "A New Standard for Radiographic Acceptance Criteria for Steel Castings," in *Proceedings of the 62nd Technical and Operating Conference,* SFSA, Chicago, IL, 2008.

2. Carlson, K., Ou, S., Hardin, R., and Beckermann, C., "Analysis of ASTM X-Ray Shrinkage Rating for Steel Castings," *Int. J. Cast Metals Research*, Vol. 14, pp. 169-183, 2001.

3. Hardin, R.A., and Beckermann, C., "A New Standard for Radiographic Acceptance Criteria for Steel Castings: Gage R&R Study," in *Proceedings of the 63rd Technical and Operating Conference,* SFSA, Chicago, IL, 2009.

4. Blair, M., Monroe, R., Hardin, R.A., and Beckermann, C., "A New Standard for Radiographic Acceptance Criteria for Steel Castings," revised May, 2010.

5. ASTM Standard E8/E8M-09, "Standard Test Methods for Tension Testing of Metallic Materials," ASTM International, West Conshohocken, PA, 2003.

6. Figliola, R., and Beasley, D., *Theory and Design for Mechanical Measurements*, 4th Ed., Wiley, 2005.

7. Montgomery, D.C., *Introduction to Statistical Quality Control*, 5th Ed., Wiley, 2005, p. 135.

8. ASM, *Tensile Testing*, 2nd Ed., Edited by J.R. Davis, ASM International, Materials Park, OH, 2003, p. 43.